msp

Algebraic & Geometric Topology 19 (2019) 397–456

Arrow calculus for welded and classical links

JEAN-BAPTISTE MEILHAN
AKIRA YASUHARA

We develop a calculus for diagrams of knotted objects. We define arrow presentations, which encode the crossing information of a diagram into arrows in a way somewhat similar to Gauss diagrams, and more generally w–tree presentations, which can be seen as "higher-order Gauss diagrams". This arrow calculus is used to develop an analogue of Habiro's clasper theory for welded knotted objects, which contain classical link diagrams as a subset. This provides a "realization" of Polyak's algebra of arrow diagrams at the welded level, and leads to a characterization of finite-type invariants of welded knots and long knots. As a corollary, we recover several topological results due to Habiro and Shima and to Watanabe on knotted surfaces in 4–space. We also classify welded string links up to homotopy, thus recovering a result of the first author with Audoux, Bellingeri and Wagner.

57M25, 57M27

Dedicated to Professor Shin'ichi Suzuki on his 77th birthday

1 Introduction

A Gauss diagram is a combinatorial object, introduced by M Polyak and O Viro [29] and T Fiedler [8], which faithfully encodes 1–dimensional knotted objects in 3–space. To a knot diagram, one associates a Gauss diagram by connecting, on a copy of S^1, the two preimages of each crossing by an arrow, oriented from the over- to the under-passing strand and labeled by the sign of the crossing. Gauss diagrams form a powerful tool for studying knots and their invariants. In particular, a result of M Goussarov [9] states that any finite-type (Goussarov–Vassiliev) knot invariant admits a Gauss diagram formula, ie can be expressed as a weighted count of arrow configurations in a Gauss diagram. A remarkable feature of this result is that, although it concerns classical knots, its proof heavily relies on *virtual knot theory*. Indeed, Gauss diagrams are inherently related to virtual knots, since an arbitrary Gauss diagram doesn't always represent a classical knot, but a virtual one; see Goussarov, Polyak and Viro [9] and Kauffman [20].

Published: 6 February 2019 DOI: 10.2140/agt.2019.19.397

More recently, further topological applications of virtual knot theory arose from its *welded* quotient, where one allows a strand to pass over a virtual crossing; see Fenn, Rimányi and Rourke [7]. This quotient is completely natural from the virtual knot group viewpoint, which naturally satisfies this additional local move. Hence, all virtual invariants derived from the knot group, such as the Alexander polynomial or Milnor invariants, are intrinsically invariants of welded knotted objects. Welded theory is also natural by the fact that classical knots and (string) links can be "embedded" in their welded counterparts. The topological significance of welded theory was enlightened by S Satoh [30]; building on early work of T Yajima [32], he defined the so-called Tube map, which "inflates" welded diagrams into ribbon knotted surfaces in dimension 4. Using the Tube map, welded theory was successfully used by B Audoux, P Bellingeri, J-B Meilhan and E Wagner [1] to classify ribbon knotted annuli and tori up to link-homotopy (for knotted annuli, it was later shown that the ribbon case can be used to give a general link-homotopy classification; see Audoux, Meilhan and Wagner [3]).

In this paper, we develop an *arrow calculus* for welded knotted objects, which can be regarded as a kind of "higher-order Gauss diagram" theory. We first recast the notion of Gauss diagram into so-called *arrow presentations* for classical and welded knotted objects. Unlike Gauss diagrams, which are "abstract" objects, arrow presentations are planar immersed arrows which "interact" with knotted diagrams. They satisfy a set of *arrow moves*, which we prove to be complete, in the following sense:

Theorem 1 (Theorem 4.5) *Two arrow presentations represent equivalent diagrams if and only if they are related by arrow moves.*

We stress that arrow moves involve no "compatibility condition", in terms of arrow signs or local strands orientations, which offers a nice contrast with the usual formulation of Gauss diagram analogues of Reidemeister moves; see [9].

The main advantage of this calculus, however, is that it generalizes to "higher orders". This relies on the notion of w*–tree presentation*, where arrows are generalized to oriented trees, which can thus be thought of as "higher-order Gauss diagrams". Arrow moves are then extended to a calculus of w*–tree moves*, ie we have a w–tree version of Theorem 1.

Arrow calculus should also be regarded as a welded version of Goussarov–Habiro theory [13; 10], solving partially a problem set by Polyak [26, Problem 2.25]. K Habiro [13] introduced the notion of clasper for (classical) knotted objects, which is a kind of

embedded graph carrying a surgery instruction. A striking result is that clasper theory gives a topological characterization of the information carried by finite-type invariants of knots. More precisely, Habiro used claspers to define the C_k–equivalence relation, for any integer $k \geq 1$, and showed that two knots share all finite-type invariants up to degree $< k$ if and only if they are C_k–equivalent. This result was also independently obtained by Goussarov [10]. In the present paper, we use w–tree presentations to define a notion of w_k–equivalence. We observe that two w_k–equivalent welded knotted objects share all finite-type invariants of degree $< k$, and prove that the converse holds for welded knots and long knots. More precisely, we use arrow calculus to show the following:

Theorem 2 (Theorem 8.1 and Corollary 8.2) *Any welded knot is* w_k*–equivalent to the unknot for* any $k \geq 1$. *Hence, there is no nontrivial finite-type invariant of welded knots.*

Theorem 3 (Corollary 8.6) *The following assertions are equivalent for any* $k \geq 1$:

(1) *Two welded long knots are* w_k*–equivalent.*

(2) *Two welded long knots share all finite-type invariants of degree* $< k$.

(3) *Two welded long knots have the same invariants* $\{\alpha_i\}$ *for* $2 \leq i < k$.

Here, the invariants α_i are given by the coefficients of the power series expansion at $t = 1$ of the normalized Alexander polynomial.

From the finite-type point of view, w–trees can thus be regarded as a "realization" of the space of oriented diagrams introduced by D Bar-Natan and Z Dancso [5], where the universal invariant of welded (long) knots takes its values, and which is a quotient of the Polyak algebra [27]. This is similar to clasper theory, which provides a topological realization of Jacobi diagrams. See Sections 10.3 and 10.6 for further comments.

We note that Theorem 2 and the equivalence (2) $\Longleftrightarrow$ (3) of Theorem 3 were independently shown for *rational-valued* finite-type invariants by Bar-Natan and Dancso [5]. Our results hold in the general case, ie for invariants valued in any abelian group. We also show that welded long knots up to w_k–equivalence form a finitely generated free abelian group; see Corollary 8.8.

Using Satoh's Tube map, we can promote these results to topological ones. More precisely, we obtain that there is no nontrivial finite-type invariant of ribbon torus

knots (Corollary 8.3), and reprove a result of Habiro and A Shima [16], stating that finite-type invariants of ribbon 2–knots are determined by the (normalized) Alexander polynomial (Corollary 8.7). Moreover, we show that Theorem 3 implies a result of T Watanabe [31], which characterizes topologically finite-type invariants of ribbon 2–knots. See Section 10.2.

We also develop a version of arrow calculus *up to homotopy*. Here, the notion of homotopy for welded diagrams is generated by the *self-(de)virtualization move*, which replaces a classical crossing between two strands of a same component by a virtual one, or vice-versa. We use the homotopy arrow calculus to prove the following.

Theorem 4 (Corollary 9.5) *Welded string links are classified up to homotopy by welded Milnor invariants.*

This result, which is a generalization of Habegger and Lin's classification of string links up to link-homotopy [11], was first shown by Audoux, Bellingeri, Wagner and the first author in [1]. Our version is stronger in that it gives, in terms of w–trees and welded Milnor invariants, an explicit representative for the homotopy class of a welded string link; see Theorem 9.4. Moreover, this result can be used to give homotopy classifications of ribbon annuli and torus links, as shown in [1].

The rest of this paper is organized as follows.

We recall in Section 2 the basics on classical and welded knotted objects, and the connection to ribbon knotted objects in dimension 4. In Section 3, we give the main definition of this paper, introducing w–arrows and w–trees. We then focus on w–arrows in Section 4. We define arrow presentations and arrow moves, and prove Theorem 1. The relation to Gauss diagrams is also discussed in more details in Section 4.4. Next, in Section 5 we turn to w–trees. We define the expansion move (E), which leads to the notion of w–tree presentation, and we provide a collection of moves on such presentations. In Section 6, we give the definitions and some properties of the welded extensions of the knot group, the normalized Alexander polynomial, and Milnor invariants. We also review the finite-type invariant theory for welded knotted objects. The w_k–equivalence relation is introduced and studied in Section 7. We also clarify there the relation to finite-type invariants and to Habiro's C_n–equivalence. Theorems 2 and 3 are proved in Section 8. In Section 9, we consider arrow calculus up to homotopy, and prove Theorem 4. We close this paper with Section 10, where we gather several comments, questions and remarks. In particular, we prove in Section 10.2 the topological consequences of our results, stated above.

Acknowledgements The authors would like to thank Benjamin Audoux for stimulating conversations, and Haruko A Miyazawa for her useful comments. Thanks are also due to the referee for insightful comments and suggestions. This paper was completed during a visit of Meilhan at Tsuda University, Tokyo, whose hospitality and support is warmly acknowledged. Yasuhara is partially supported by a Grant-in-Aid for Scientific Research (C) (#17K05264) of the Japan Society for the Promotion of Science.

2 A quick review of classical and welded knotted objects

2.1 Basic definitions

A *classical knotted object* is the image of an embedding of some oriented 1–manifold in 3–dimensional space. Typical examples include knots and links, braids, string links and, more generally, tangles. It is well known that such embeddings are faithfully represented by a generic planar projection, where the only singularities are transverse double points endowed with a diagrammatic over/under information, as in Figure 1, left, modulo Reidemeister moves I, II and III.

This diagrammatic realization of classical knotted objects generalizes to virtual and welded knotted objects, as we briefly outline below.

A *virtual diagram* is the image of an immersion of some oriented 1–manifold in the plane, whose singularities are a finite number of transverse double points that are labeled, either as a *classical crossing* or as a *virtual crossing*, as shown in Figure 1.

Convention 2.1 We do not use here the usual drawing convention for virtual crossings, with a circle around the corresponding double point.

There are three classes of local moves that one considers on virtual diagrams:

- the three classical Reidemeister moves;
- the three virtual Reidemeister moves, which are the exact analogues of the classical ones with all classical crossings replaced by virtual ones;
- the mixed Reidemeister move, shown in Figure 2, left.

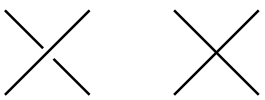

Figure 1: A classical and a virtual crossing

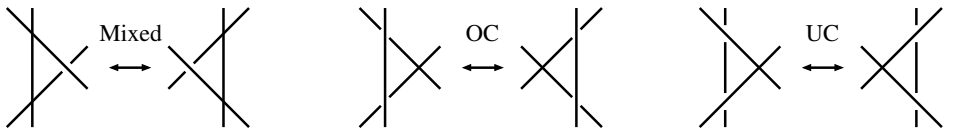

Figure 2: The mixed, OC and UC moves on virtual diagrams

We call these three classes of moves the *generalized Reidemeister moves*.

A *virtual knotted object* is the equivalence class of a virtual diagram under planar isotopy and generalized Reidemeister moves. This notion was introduced by Kauffman in [20], to which we refer the reader for a much more detailed treatment.

Recall that generalized Reidemeister moves in particular imply the so-called *detour move*, which replaces an arc passing through a number of virtual crossings by any other such arc with the same endpoints.

Recall also that there are two "forbidden" local moves, called *OC and UC moves* (for overcrossings and undercrossings commute), as illustrated in Figure 2.

In this paper, we shall instead consider the following natural quotient of virtual theory.

Definition 2.2 A *welded knotted object* is the equivalence class of a virtual diagram under planar isotopy, generalized Reidemeister moves and OC moves.

There are several reasons that make this notion both natural and interesting. The virtual knot group introduced by Kauffman [20] at the early stages of virtual knot theory is intrinsically a welded invariant. As a consequence, the virtual extensions of classical invariants derived from (quotients of) the fundamental group are in fact welded invariants; see Section 6. Another, topological motivation is the relation with ribbon knotted objects in codimension 2; see Section 2.2.

In what follows, we will be mainly interested in *welded links and welded string links*, which are the welded extensions of classical link and string link diagrams. Recall that, roughly speaking, an n–component welded string link is a diagram made of n arcs properly immersed in a square, with n points marked on the lower and upper faces, such that the k^{th} arc runs from the k^{th} lower to the k^{th} upper marked point. A 1–component string link is often called a *long knot* in the literature; we shall use this terminology here as well.

Welded (string) links are a genuine extension of classical (string) links, in the sense that the latter can be "embedded" into the former ones. This is shown strictly as in the knot case [9, Theorem 1.B], and actually also holds for virtual objects.

Convention 2.3 In the rest of this paper, by "diagram" we will implicitly mean an oriented diagram, containing classical and/or virtual crossings, and the natural equivalence relation on diagrams will be that of Definition 2.2. We shall sometimes use the terminology "welded diagram" to emphasize this fact. As noted above, this includes in particular classical (string) link diagrams.

Remark 2.4 The OC move, together with generalized Reidemeister moves, implies a welded version of the detour move, called a w*–detour move*, which replaces an arc passing through a number of over-crossings by any other such arc with the same endpoints. This is proved strictly as for the detour move.

2.2 Welded theory and ribbon knotted objects in codimension 2

As already indicated, one of the main interests of welded knot theory is that it allows one to study certain knotted surfaces in 4–space. As a matter of fact, the main results of this paper will have such topological applications, so we briefly review these objects and their connection to welded theory.

Recall that a *ribbon immersion* of a 3–manifold M in 4–space is an immersion admitting only ribbon singularities, which are 2–disks with two preimages, one being embedded in the interior of M, and the other being properly embedded.

A *ribbon 2–knot* is the boundary of a ribbon immersed 3–ball in 4–space, and a *ribbon torus knot* is, likewise, the boundary of a ribbon immersed solid torus in 4–space. More generally, by *ribbon knotted object*, we mean a knotted surface obtained as the boundary of some ribbon immersed 3–manifold in 4–space.

Using works of Yajima [32], Satoh defined in [30] a surjective *Tube map*, from welded diagrams to ribbon 2–knotted objects. Roughly speaking, the Tube map assigns, to each classical crossing of a diagram, a pair of locally linked annuli in a 4–ball, as shown in [30, Figure 6]; next, it only remains to connect these annuli to one another by unlinked annuli, as prescribed by the diagram. Although not injective in general,[1] the Tube map acts faithfully on the "fundamental group". This key fact, which will be made precise in Remark 6.1, will allow to draw several topological consequences from our diagrammatic results. See Section 10.2.

[1] The Tube map is not injective for welded knots [17], but is injective for welded braids [6] and welded string links up to homotopy [1].

Remark 2.5 One can more generally define k–dimensional ribbon knotted objects in codimension 2, for any $k \geq 2$, and the Tube map generalizes straightforwardly to a surjective map from welded diagrams to k–dimensional ribbon knotted objects. See for example [3]. As a matter of fact, most of the topological results of this paper extend freely to ribbon knotted objects in codimension 2.

3 w–arrows and w–trees

Let D be a diagram. The following is the main definition of this paper:

Definition 3.1 A w–*tree* for D is a connected uni-trivalent tree T, immersed in the plane of the diagram such that:

- The trivalent vertices of T are pairwise disjoint and disjoint from D.
- The univalent vertices of T are pairwise disjoint and are contained in $D \setminus \{\text{crossings of } D\}$.
- All edges of T are oriented, such that each trivalent vertex has two ingoing and one outgoing edge.
- We allow virtual crossings between edges of T, and between D and edges of T, but classical crossings involving T are not allowed.
- Each edge of T is assigned a number (possibly zero) of decorations $\bullet$, called *twists*, which are disjoint from all vertices and crossings, and subject to the involutive rule

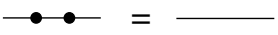

A w–tree with a single edge is called a w–*arrow*.

For a union of w–trees for D, vertices are assumed to be pairwise disjoint, and all crossings among edges are assumed to be virtual. See Figure 3 for an example.

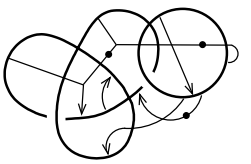

Figure 3: Example of a union of w–trees

We call *tails* the univalent vertices of T with outgoing edges, and we call the *head* the unique univalent vertex with an ingoing edge. We will call an *endpoint* any univalent vertex of T, when we do not need to distinguish between tails and head. The edge which is incident to the head is called *terminal*.

Two endpoints of a union of w–trees for D are called *adjacent* if, when traveling along D, these two endpoints are met consecutively, without encountering any crossing or endpoint.

Remark 3.2 Given a uni-trivalent tree, picking a univalent vertex as the head uniquely determines an orientation on all edges respecting the above rule. Thus, we usually only indicate the orientation on w–trees at the terminal edge. However, it will occasionally be useful to indicate the orientation on other edges, for example when drawing local pictures.

Definition 3.3 Let $k \geq 1$ be an integer. A w–*tree of degree* k — or w_k–*tree* — for D is a w–tree for D with k tails.

Convention 3.4 Diagrams are drawn with bold lines, while w–trees are drawn with thin lines. See Figure 3. We shall also use the symbol $\circ$ to describe a w–tree that *may or may not* contain a twist at the indicated edge:

4 Arrow presentations of diagrams

In this section, we focus on w–arrows. We explain how w–arrows carry "surgery" instructions on diagrams, so that they provide a way to encode diagrams. A complete set of moves is provided, relating any two w–arrow presentations of equivalent diagrams. The relation to the theory of Gauss diagrams is also discussed.

4.1 Surgery along w–arrows

Let A be a union of w–arrows for a diagram D. *Surgery along* A yields a new diagram, denoted by D_A, which is defined as follows.

Suppose that there is a disk in the plane that intersects $D \cup A$ as shown in Figure 4. The figure then represents the result of surgery along A on D. We emphasize the fact that the orientation of the portion of diagram containing the tail needs to be specified to define the surgery move.

Figure 4: Surgery along a w–arrow

If some w–arrow of A intersects the diagram D (at some virtual crossing disjoint from its endpoints), then this introduces pairs of virtual crossings as indicated on the left-hand side of the figure below. Likewise, the right-hand side of the figure indicates the rule when two portions of (possibly the same) w–arrow(s) of A intersect:

Finally, if some w–arrow of A contains some twists, we simply insert virtual crossings accordingly, as indicated below:

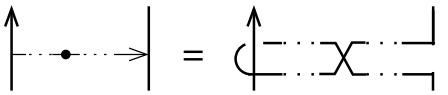

Note that this is compatible with the involutive rule for twists by the virtual Reidemeister II move, as shown below:

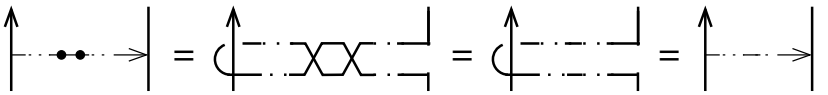

Note also that, for a dotted arrow whose interior is disjoint from the diagram and all other arrows, surgery reformulates as follows:

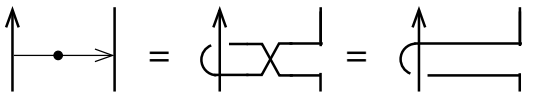

An example is given in Figure 5.

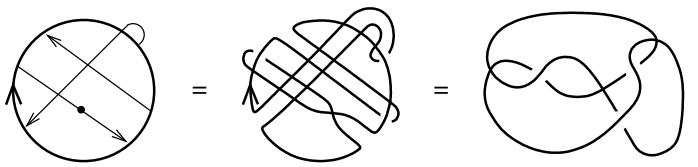

Figure 5: An example of a diagram obtained by surgery along w–arrows

4.2 Arrow presentations

Having defined surgery along w–arrows, we are led to the following:

Definition 4.1 An *arrow presentation* for a diagram D is a pair (V, A) of a diagram V *without classical crossings* and a collection of w–arrows A for V such that surgery on V along A yields the diagram D.

We say that two arrow presentations are *equivalent* if the surgeries yield equivalent diagrams. We will simply denote this equivalence by $=$.

In the next section, we address the problem of generating this equivalence relation by local moves on arrow presentations.

As Figure 6 illustrates, surgery along a w–arrow is equivalent to a *devirtualization move*, which is a local move that replaces a virtual crossing by a classical one.

Figure 6: Surgery along a w–arrow is a devirtualization move.

This observation implies the following:

Proposition 4.2 *Any diagram admits an arrow presentation.*

More precisely, for a diagram D, there is a uniquely defined arrow presentation (V_D, A) which is obtained by applying the rule of Figure 6 at each (classical) crossing. Note that V_D is obtained from D by replacing all classical crossings by virtual ones.

Definition 4.3 We call the pair (V_D, A) the *canonical arrow presentation* of the diagram D.

For example, for the diagram of the trefoil shown in Figure 16, the canonical arrow presentation is given in the center of the figure.

4.3 Arrow moves

Arrow moves are the following six types of local moves among arrow presentations:

(1) **Virtual isotopy** Virtual Reidemeister moves involving edges of w–arrows and/or strands of diagram, together with the following local moves:[2]

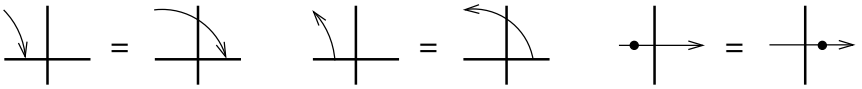

(2) **Head/tail reversal**

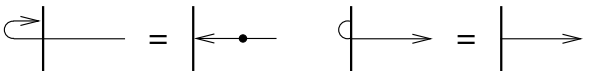

(3) **Tails exchange**

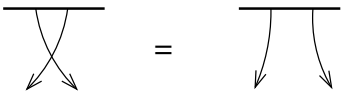

(4) **Isolated arrow**

(5) **Inverse**

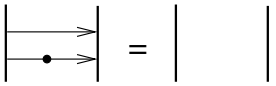

(6) **Slide**

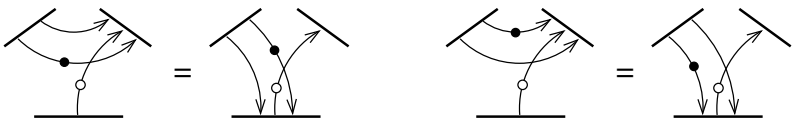

Lemma 4.4 *Arrow moves yield equivalent arrow presentations.*

Proof Virtual isotopy moves (1) are easy consequences of the surgery definition of w–arrows and virtual Reidemeister moves. This is clear for the Reidemeister-type moves, since all such moves locally involve only virtual crossings. The remaining local

[2]Here, in the figures, the vertical strand is either a portion of diagram or of a w–arrow.

moves essentially follow from detour moves. For example, the figure below illustrates the proof of one instance of the second move, for one choice of orientation at the tail:

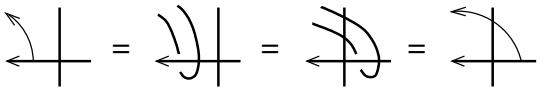

All other moves of (1) are given likewise by virtual Reidemeister moves.

Having proved this first sets of moves, we can freely use them to simplify the proof of the remaining moves. For example, we can freely assume that the w–arrow involved in the reversal move (2) is either as shown in Figure 7, left, or differs from this figure by a single twist. The proof of the tail reversal move is given in Figure 7 in the case where the w–arrow has no twist and the strand is oriented upwards (in the figure of the tail reversal move (2)).

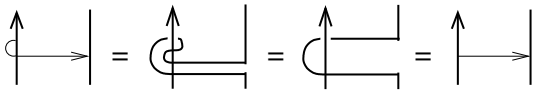

Figure 7: Proving the tail reversal move

It only uses the definition of a w–arrow and the virtual Reidemeister II move. The other cases are similar, and left to the reader.

Likewise, we only prove head reversal in Figure 8 when the w–arrow has no twist. Note that the tail reversal and isotopy moves allow us to chose the strand orientation as depicted. The identities in the figure follow from elementary applications of generalized Reidemeister moves.

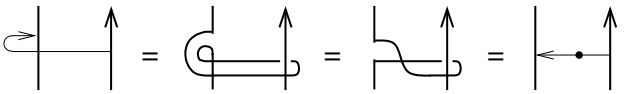

Figure 8: Proving the head reversal move

Figure 9 shows (3). There, the second and fourth identities are applications of the detour move, while the third move uses the OC move. In Figure 9, we had to choose a local orientation for the upper strand. This implies the result for the other choice of orientation, by using the tail reversal move (2).

Moves (4) and (5) are direct consequences of the definition, and are left to the reader.

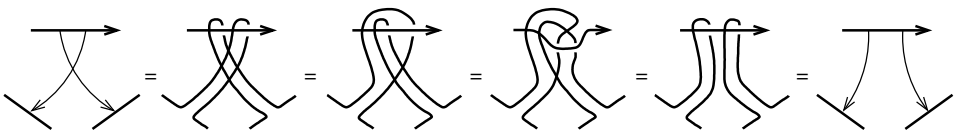

Figure 9: Proving the tails exchange move

Finally, we prove (6). We only show here the first version of the move, the second one being strictly similar. There are a priori several choices of local orientations to consider, which are all dealt with in two versions, depending on whether we insert a twist on the $\circ$–marked w–arrow or not. Figure 10 illustrates the proof for one choice of orientation, in the case where no twist is inserted. The sequence of identities in this figure is given as follows: the second and third identities use isotopies and detour moves, the fourth (vertical) one uses the w–detour move, then followed by isotopies and detour moves which give the fifth equality. The final step uses the tails exchange move (3).

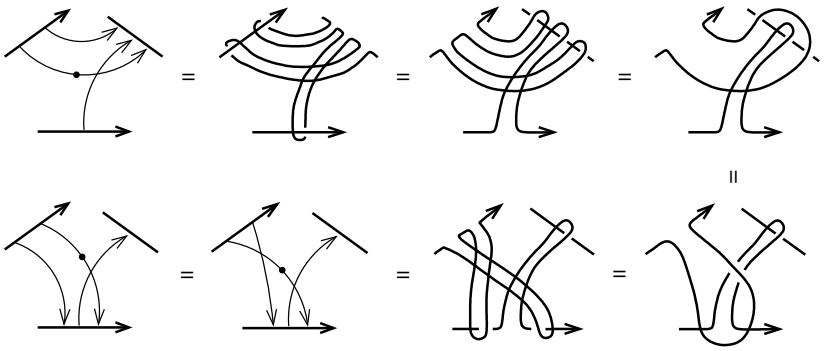

Figure 10: Proving the slide move

Now, notice that the exact same proof applies in the case where there is a twist on the $\circ$–marked w–arrow. Moreover, if we change the local orientation of, say, the bottom strand in the figure, the result follows from the previous case by the reversal move (2), the tails exchange move (3) and twist involutivity, as the following picture indicates:

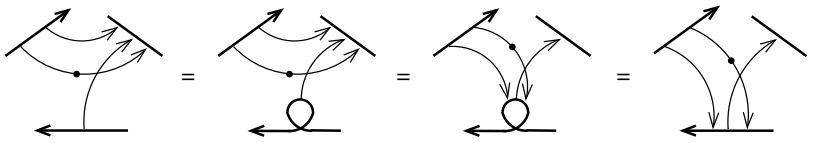

We leave it to the reader to check that, similarly, all other choices of local orientations follow from the first one. □

The main result of this section is that this set of moves is complete.

Theorem 4.5 *Two arrow presentations represent equivalent diagrams if and only if they are related by arrow moves.*

The *if* part of the statement is shown in Lemma 4.4. In order to prove the *only if* part, we will need the following:

Lemma 4.6 *If two diagrams are equivalent, then their canonical arrow presentations are related by arrow moves.*

Proof It suffices to show that generalized Reidemeister moves and OC moves are realized by arrow moves among canonical arrow presentations.

Virtual Reidemeister moves and the mixed move follow from virtual isotopy moves (1). For example, the case of the mixed move is illustrated in Figure 11 (the argument holds for any choice of orientation).

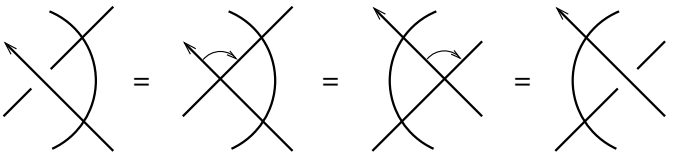

Figure 11: Realizing the mixed move by arrow moves

The OC move is, as expected, essentially a consequence of the tails exchange move (3). More precisely, Figure 12 shows how applying the tails exchange together with isotopy moves (1), followed by tail reversal moves (2) and further isotopy moves, realizes the OC move.

Figure 12: Realizing the OC move by arrow moves

We now turn to classical Reidemeister moves. The proof for the Reidemeister I move is illustrated in Figure 13. There, the second equality uses move (1), while the third equality uses the isolated arrow move (4). (More precisely, one has to consider both orientations in the figure, as well as the opposite crossing, but these other cases are similar.)

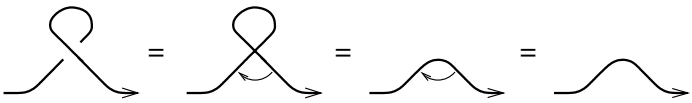

Figure 13: Realizing the Reidemeister I move by arrow moves

The proof for the Reidemeister II move is shown in Figure 14, where the second equality uses moves (1) and the head reversal move (2), and the third equality uses the inverse move (5).

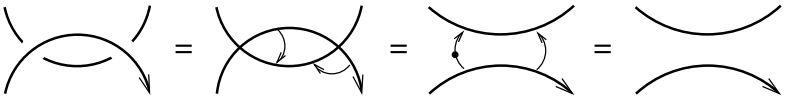

Figure 14: Realizing the Reidemeister II move by arrow moves

Finally, for the Reidemeister move III, we first note that, although there are a priori eight choices of orientation to be considered, Polyak showed that only one is necessary [28]. We consider this move in Figure 15.

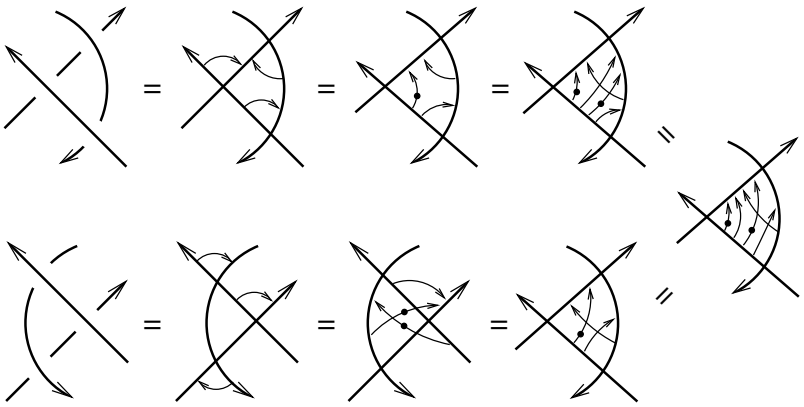

Figure 15: Realizing the Reidemeister III move by arrow moves

There, the second equality uses the reversal and isotopy moves (2) and (1), the third equality uses the inverse move (5) and the fourth one uses the slide move (6) as well as the tails exchange move (3). Then the fifth equality uses the inverse move back again, the sixth equality uses the reversal, isotopy and tails exchange moves, and the seventh one uses further reversal and isotopy moves. □

Remark 4.7 We note from the above proof that some of the arrow moves appear as essential analogues of the generalized Reidemeister moves: the isolated move (4) gives Reidemeister I move, while the inverse move (5) and slide move (6) give Reidemeister II and III, respectively. Finally, the tails exchange move (3) corresponds to the OC move.

We can now prove the main result of this section.

Proof of Theorem 4.5 As already mentioned, it suffices to prove the *only if* part. Observe that, given a diagram D, any arrow presentation of D is equivalent to the canonical arrow presentation of some diagram. Indeed, by the involutivity of twists and the head reversal move (2), we can assume that the arrow presentation of D contains no twist. We can then apply isotopy and tail reversal moves (1) and (2) to assume that each w–arrow is contained in a disk as in Figure 4, left; by using virtual Reidemeister moves II, we can actually assume that it is next to a (virtual) crossing, as in Figure 6, left. The resulting arrow presentation is thus a canonical arrow presentation of some diagram (which is equivalent to D, by Lemma 4.4).

Now, consider two equivalent diagrams, and pick any arrow presentations for these diagrams. By the previous observation, these arrow presentations are equivalent to canonical arrow presentations of equivalent diagrams. The result then follows from Lemma 4.6. □

4.4 Relation to Gauss diagrams

Although similar-looking and closely related, w–arrows are not to be confused with arrows of Gauss diagrams. In particular, the signs on arrows of a Gauss diagram are not equivalent to twists on w–arrows. Indeed, the sign of the crossing defined by a w–arrow relies on the local orientation of the strand where its head is attached. The local orientation at the tail, however, is irrelevant. Let us clarify here the relationship between these two objects.

Given an arrow presentation (V, A) for some diagram K (of, say, a knot) one can always turn it by arrow moves into an arrow presentation (V_0, A_0), where V_0 is a trivial diagram, with no crossing. See for example the case of the trefoil in Figure 16.

There is a unique Gauss diagram for K associated to (V_0, A_0), which is simply obtained by the following rule. First, each w–arrow in A_0 inherits a sign, which is $+$ (resp. $-$) if, when running along V_0 following the orientation, the head is attached to the right-hand (resp. left-hand) side. Next, change this sign if and only if the w–arrow

Figure 16: The right-handed trefoil as obtained by surgery on w–arrows

contains an odd number of twists. For example, the Gauss diagram for the right-handed trefoil shown in Figure 16 is obtained from the arrow presentation on the right-hand side by labeling all three arrows by $+$. Note that, if the head of a w–arrow is attached to the right-hand side of the diagram, then the parity of the number of twists corresponds to the sign.

Conversely, any Gauss diagram can be converted to an arrow presentation, by attaching the head of an arrow to the right-hand (resp. left-hand) side of the (trivial) diagram if it is labeled by a $+$ (resp. $-$).

Theorem 4.5 provides a complete calculus (arrow moves) for this alternative version of Gauss diagrams (arrow presentations), which is to be compared with the Gauss diagram versions of Reidemeister moves. Although the set of arrow moves is larger, and hence less suitable for (say) proving invariance results, it is in general much simpler to manipulate. Indeed, the usual formulation of the Gauss diagram versions of Reidemeister moves III, as given in [9], contains rather delicate compatibility conditions, given by both the arrow signs and local orientations of the strands. Arrow moves, on the other hand, involve no such condition; actually, what our work suggests is that the Reidemeister III move can be given a Gauss diagram version, similar in flavor to the slide move (6), which can be formulated without any restriction. Moreover, we shall see in the next sections that arrow calculus generalizes widely to w–trees. This can thus be seen as an "higher-order Gauss diagram" calculus.

5 Surgery along w–trees

In this section, we show how w–trees allow us to generalize surgery along w–arrows.

5.1 Subtrees, expansion, and surgery along w–trees

We start with a couple of preliminary definitions.

A *subtree* of a w–tree is a connected union of edges and vertices of this w–tree (a valence two vertex being assumed to be a point of a single edge).

Given a subtree S of a w–tree T for a diagram D (possibly T itself), consider for each endpoint e of S a point e' on D, which is adjacent to e, such that e and e' are met consecutively, in this order, when running along D following the orientation. One can then form a new subtree S', by joining these new points by the same directed subtree as S, so that it runs parallel to it and crosses it only at virtual crossings. We then say that S and S' are two *parallel subtrees*.

We now introduce the *expansion move* (E), which comes in two versions as shown in Figure 17.

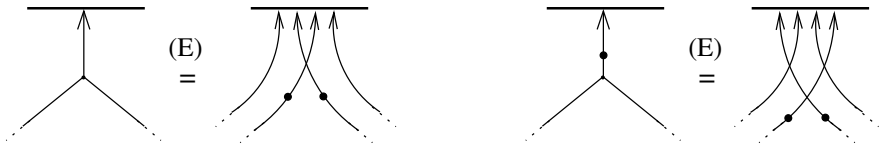

Figure 17: Expanding w–trees by using (E)

Convention 5.1 In Figure 17, the dotted lines on the left-hand side of the equality represent two subtrees, forming, along with the part which is shown, a w–tree. The dotted parts on the right-hand side then represent parallel copies of both subtrees. Together with the represented part, they form pairs of parallel w–trees which only differ by a twist on the terminal edge. See the first equality of Figure 18 for an example. We shall use this diagrammatic convention throughout the paper.

By applying (E) recursively, we can eventually turn any w–tree into a union of w–arrows. Note that this process is uniquely defined. An example is given in Figure 18.

Definition 5.2 The *expansion* of a w–tree is the union of w–arrows obtained from repeated applications of (E).

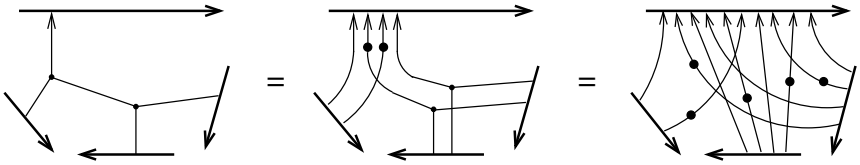

Figure 18: Expansion of a w_3–tree

Remark 5.3 As Figure 18 illustrates, the expansion of a w_k–tree T takes the form of an "iterated commutators of w–arrows". More precisely, labeling the tails of T

from 1 to k, and denoting by i a w–arrow running from (a neighborhood of) tail i to (a neighborhood of) the head of T, and by i^{-1} a similar w–arrow with a twist, the heads of the w–arrows in the expansion of T are met along D according to a k–fold commutator in $1, \dots, k$. See Section 6.1.2 for a more rigorous and detailed treatment.

The notion of expansion leads to the following:

Definition 5.4 The *surgery along a* w*–tree* is the surgery along its expansion.

As before, we shall denote by D_T the result of surgery on a diagram D along a union T of w–trees.

We have the following *Brunnian-type property*:

Proposition 5.5 *Given a* w*–tree T, consider the trivial tangle D given by a neighborhood of its endpoints; the tangle D_T is Brunnian, in the sense that deleting any component yields a trivial tangle.*

Proof First, observe that D_T is clearly trivialized when deleting the component corresponding to the head of T. So it suffices to show that this is also true when deleting a component corresponding to any tail of T, which can be done by induction on the degree of T. The case where T is a w–arrow is obvious. Now, for a w–tree T of higher degree, applying the expansion move (E) yields four w–trees of lower degree, as illustrated in Figure 17, and the result follows by combining the induction hypothesis and the inverse move lemma, Lemma 5.9 below. □

5.2 Moves on w–trees

In this section, we extend the arrow calculus set up in Section 4 to w–trees. The expansion process, combined with Lemma 4.4, gives immediately the following:

Lemma 5.6 *Arrow moves* (1)–(4) *hold for* w*–trees as well. More precisely*:

- *One should add the following local moves to* (1):

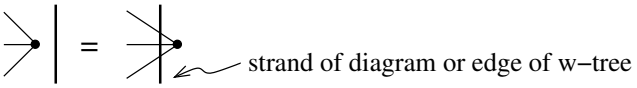

- *The tails exchange move* (3) *may involve tails from different components or from a single component.*

Remark 5.7 As a consequence of the tails exchange move for w–trees, the relative position of two (sub)trees for a diagram is completely specified by the relative position of the two heads. In particular, we can unambiguously refer to *parallel* w*–trees* by only specifying the relative position of their heads. Likewise, we can freely refer to "parallel subtrees" of two w–trees if these subtrees do not contain the head.

Convention 5.8 In the rest of the paper, we will use the same terminology for the w–tree versions of moves (1)–(4), and in particular we will use the same numbering. As for moves (5) and (6), we will rather refer to the next two lemmas when used for w–trees.

As a generalization of the inverse move (5), we have the following:

Lemma 5.9 (inverse) *Two parallel* w*–trees which only differ by a twist on the terminal edge yield a trivial surgery:*

Proof We only prove here the first equality, the second one being strictly similar. We proceed by induction on the degree of the w–trees involved. The w–arrow case is given by move (5). Now, suppose that the left-hand side in the above figure involves two w_k–trees. Then, one can apply (E) to both to obtain a union of eight w–trees of degree $< k$. Figure 19 then shows how repeated use of the induction hypothesis implies the result. □

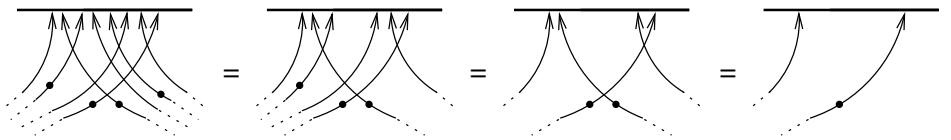

Figure 19: Proving the inverse move for w–trees

Convention 5.10 In the rest of this paper, when given a union S of w–trees with adjacent heads, we will denote by $\overline{S}$ the union of w–trees such that we have

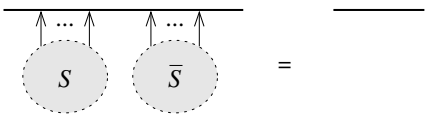

Note that $\overline{S}$ can be described explicitly from S, by using Lemma 5.9 recursively. We stress that the above graphical convention will always be used for w–trees with adjacent heads, so that no tail is attached to the represented portion of diagram.

Likewise, we have the following natural generalization of the slide move (6):

Lemma 5.11 (slide move for w–trees) *The following equivalence holds:*

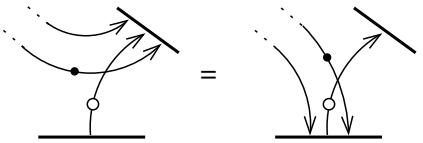

Proof The proof is done by induction on the degree of the w–trees involved in the move, as in the proof of Lemma 5.9. The degree 1 case is the slide move (6) for w–arrows. Now, suppose that the left-hand side in the figure of Lemma 5.11 involves two w_k–trees, and apply (E) to obtain a union of eight w–trees of degree $< k$. These w–trees are such that we can slide them pairwise, using the induction hypothesis four times. Applying (E) back again to the resulting eight w–trees, we obtain the desired pair of w_k–trees. □

Remark 5.12 The slide lemma, Lemma 5.11, generalizes as follows. If one replaces the w–arrow in Lemma 5.11 by a bunch of parallel w–arrows, then the lemma still applies. Indeed, it suffices to insert, using Lemma 5.9 (inverse), pairs of parallel w–trees between the endpoints of each pair of consecutive w–arrows, apply Lemma 5.11 and then remove pairwise all the added w–trees again by the inverse lemma. Note that this applies for any parallel bunch of w–arrows, for any choice of orientation and twist on each individual w–arrow.

We now provide several supplementary moves for w–trees.

Lemma 5.13 (head traversal) *A w–tree head can pass through an isolated union of w–trees:*[3]

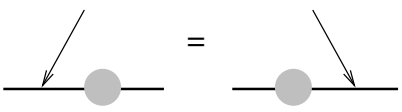

[3] In the figure, the shaded part indicates a portion of the diagram with some w–trees, which is contained in a disk as shown.

Proof Clearly, by (E), it suffices to prove the result for a w–arrow head. The proof is given in Figure 20. (More precisely, the figure proves the equality for one choice of orientation; the other case is strictly similar.)

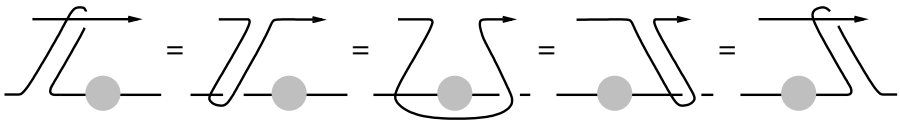

Figure 20: Proving the head traversal move

Surgery yields the diagram shown on the left-hand side of the figure, which can be deformed into the second diagram by a planar isotopy. Successive applications of the detour move and of the w–detour move (Remark 2.4) then give the next two equalities, and another planar isotopy completes the proof. □

Lemma 5.14 (heads exchange) *Exchanging two heads can be achieved at the expense of an additional* w*–tree, as shown below:*

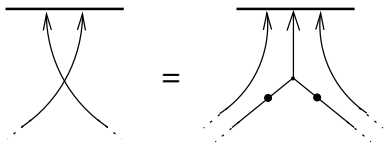

Proof Starting from the right-hand side of the above equality, applying the expansion move (E) gives the first equality in Figure 21. The involutivity of twists gives the second equality, and two applications of Lemma 5.9 (inverse) then conclude the proof. □

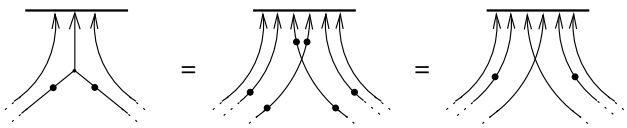

Figure 21: Proving the heads exchange move

Remark 5.15 By strictly similar arguments, one can show the simple variants of the heads exchange move given in Figure 22.

Lemma 5.16 (head–tail exchange) *Exchanging a* w*–tree head and a* w*–arrow tail can be achieved at the expense of an additional* w*–tree, as shown in Figure 23.*

Proof We only prove the version of the equality where there is no twist on the left-hand side, the other one being strictly similar. The proof is given in Figure 24.

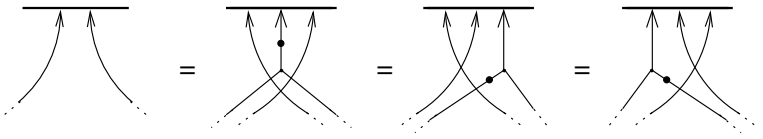

Figure 22: Some variants of the heads exchange move

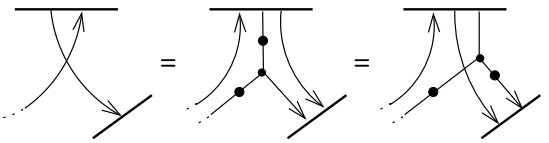

Figure 23: The head–tail exchange move

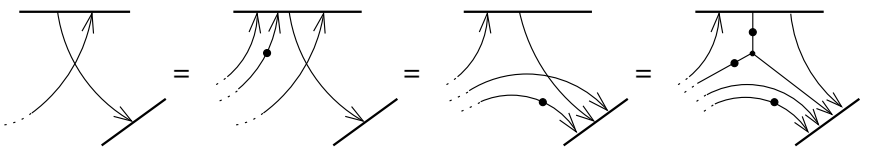

Figure 24: Proving the head–tail exchange move

The three identities depicted there respectively use Lemmas 5.9 (inverse), 5.11 (slide) and 5.14 (heads exchange). Another application of the inverse lemma then concludes the argument. □

Lemma 5.17 (antisymmetry) *The cyclic order at a trivalent vertex, induced by the plane orientation, may be changed at the cost of a twist on the three incident edges:*

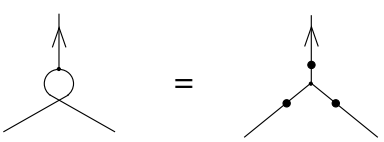

Proof The proof is by induction on the number of edges from the head to the trivalent vertex involved in the move. When there is only one edge, the result simply follows from (E), isotopy of the resulting w–trees and (E) back again, as shown in Figure 25. (Here, we only show the case where the terminal edge contains no twist; the other case is similar.) In the general case, we use (E) to apply the induction hypothesis to the resulting w–trees, and use (E) back again, as in the proofs of Lemmas 5.9 and 5.11. □

A *fork* is a subtree which consists of two adjacent tails connected to the same trivalent vertex (possibly containing some twists). See Figure 26.

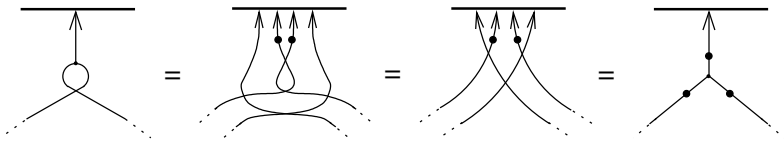

Figure 25: Proving the antisymmetry lemma

Lemma 5.18 (fork move) *Surgery along a* w*–tree containing a fork does not change the equivalence class of a diagram.*

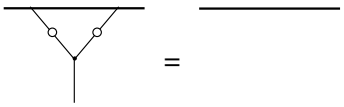

Figure 26: The fork move

Proof The proof is by induction on the number of edges from the head to the fork. The initial case of a w_2–tree with adjacent tails is shown in Figure 27, in the case where no edge contains a twist (the other cases are similar).

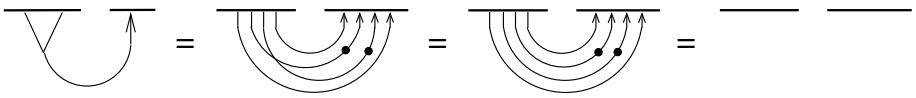

Figure 27: Proving the fork move

The inductive step is clear: applying (E) to a w–tree containing a fork yields four w–trees, two of which contain a fork, by the tails exchange move (3). Using the induction hypothesis, we are thus left with two w–trees, which cancel by Lemma 5.9 (inverse). □

5.3 w–tree presentations for welded knotted objects

We have the following natural generalization of the notion of arrow presentation:

Definition 5.19 Suppose that a diagram is obtained from a diagram V *without* classical crossings by surgery along a union T of w–trees. Then (V, T) is called a w*–tree presentation* of the diagram.

Two w–tree presentations are *equivalent* if they represent equivalent diagrams.

Let us call w–*tree moves* the set of moves on w–trees given by the results of Section 5. More precisely, w–tree moves consists of the expansion move (E), Moves (1)–(4) of Lemma 5.6, and the inverse (Lemma 5.9), slide (Lemma 5.11), head traversal (Lemma 5.13), heads exchange (Lemma 5.14), head–tail exchange (Lemma 5.16), antisymmetry (Lemma 5.17) and fork (Lemma 5.18) moves. Clearly, w–tree moves yield equivalent w–tree presentations.

Examples of w–tree presentations for the right-handed trefoil are given in Figure 28. There, starting from the arrow presentation of Figure 16, we apply Lemma 5.16 (head–tail exchange), the tails exchange move (3) and the isolated arrow move (4).

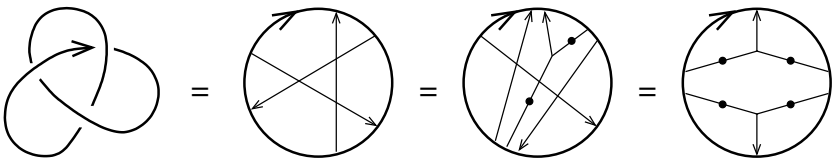

Figure 28: Tree presentation for the trefoil

As mentioned in Section 4.4, these can be regarded as kinds of "higher-order Gauss diagram" presentations for the trefoil.

Remark 5.20 As pointed out to the authors by D Moussard, Figure 28 shows that the trefoil can be written as a composite knot when seen as a welded object (note, however, that connected sum is not well defined for welded knots). Actually, it follows from the fork lemma, Lemma 5.18, that the two factors are equivalent to the unknot, meaning that the trefoil is, rather surprisingly, the composite of two unknots. In fact, we can show, using bridge presentations and arrow calculus, that this is the case for *any* 2–bridge knot.

It follows from Theorem 4.5 that w–tree moves provide a complete calculus for w–tree presentations. In other words, we have the following:

Theorem 5.21 *Two* w*–tree presentations represent equivalent diagrams if and only if they are related by* w*–tree moves.*

Note that the set of w–tree moves is highly nonminimal. In fact, the above remains true when only considering the expansion move (E) and arrow moves (1)–(6).

6 Welded invariants

In this section, we review several welded extensions of classical invariants.

6.1 Virtual knot group

Let L be a welded (string) link diagram.

Recall that the *group* $G(L)$ *of* L is defined by a Wirtinger presentation, as follows. Each arc of L (ie each piece of strand bounded by either a strand endpoint or an underpassing arc in a classical crossing) yields a generator, and each classical crossing gives a relation, as indicated in Figure 29.

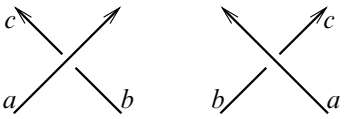

Figure 29: Wirtinger relation at each crossing

Since virtual crossings do not produce any generator or relation, virtual and mixed Reidemeister moves obviously preserve the group presentation [20]. It turns out that this "virtual knot group" is also invariant under the OC move, and is thus a welded invariant [20; 30].

6.1.1 Wirtinger presentation using w–trees Given a w–tree presentation of a diagram L, we can associate a Wirtinger presentation of $G(L)$ which involves in general fewer generators and relations. More precisely, let (V, T) be a w–tree presentation of L, where $T = T_1 \cup \cdots \cup T_r$ has r connected components. The r heads of T split V into a collection of n arcs,[4] and we pick a generator m_i for each of them. Consider the free group F generated by these generators, where the inverse of a generator m_i will be denoted by $\overline{m}_i$. Arrange the heads of T (applying the head reversal move (2) if needed) so that it looks locally as in Figure 30. Then we have

$$G(L) = \langle \{m_i\}_i \mid R_j \ (j = 1, \dots, r) \rangle,$$

where R_j is a relation associated with T_j as illustrated in the figure. There, $w(T_j)$ is a word in F, constructed as follows.

[4]More precisely, the heads of T split V into a collections of arcs and possibly several circles, corresponding to closed components of V with no head attached.

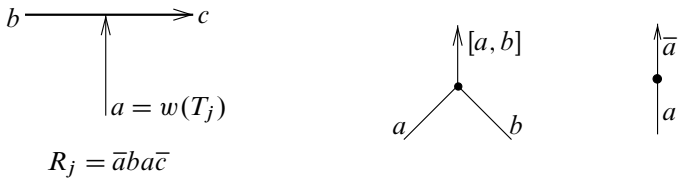

Figure 30: Wirtinger-type relation at a head and the procedure to define $w(T)$

First, label each edge of T_j which is incident to a tail by the generator m_i inherited from its attaching point. Next, label all edges of T_j by elements of F by applying recursively the rules illustrated in Figure 30. More precisely, assign recursively to each outgoing edge at a trivalent vertex the formal bracket

$$[a, b] := a\bar{b}\bar{a}b,$$

where a and b are the labels of the two ingoing edges, following the plane orientation around the vertex; we also require that a label meeting a twist is replaced by its inverse. This procedure yields a word $w(T_j) \in F$ associated to T_j, which is defined as the label at its terminal edge. Note that this procedure more generally associates a formal word to any subtree of T_j, and that, by the tail reversal move (2), the local orientation of the diagram at each tail is not relevant in this process.

In the case of a canonical arrow presentation of a diagram, the above procedure recovers the usual Wirtinger presentation of the diagram, and it is easily checked that, in general, this procedure indeed gives a presentation of the same group.

Remark 6.1 As outlined in Section 2.2, the Tube map that "inflates" a welded diagram L into a ribbon knotted surface acts faithfully on the virtual knot group, in the sense that we have an isomorphism $G(L) \cong \pi_1(\mathrm{Tube}(L))$,[5] which maps meridians to meridians and (preferred) longitudes to (preferred) longitudes, so that the Wirtinger presentations are in one-to-one correspondence; see [30; 32; 1].

6.1.2 Algebraic formalism for w–trees Let us push a bit further the algebraic tool introduced in the previous section.

Given two w–trees T and T' with adjacent heads in a w–tree presentation, which locally are arranged as in Figure 30, and are such that the head of T is met before that

[5]Here, $\pi_1(\mathrm{Tube}(L))$ denotes the fundamental group of the complement of the surface $\mathrm{Tube}(L)$ in 4–space.

of T' when following the orientation, we define

$$w(T \cup T') := w(T)w(T') \in F.$$

Convention 6.2 Here F denotes the free group on the set of Wirtinger generators of the given w–tree presentation, as defined in Section 6.1.1. In what follows, we will always use this implicit notation.

Note that, if $\overline{T}$ is obtained from T by inserting a twist in its terminal edge, then $w(\overline{T}) = \overline{w(T)}$, and $w(T \cup \overline{T}) = 1$, which is compatible with Convention 5.10.

Now, if we denote by $E(T)$ the result of one application of (E) to some w–tree T, then we have $w(T) = w(E(T))$. More precisely, if we simply denote by A and B the words associated with the two subtrees at the two ingoing edges of the vertex where (E) is applied, then we have

$$w(T) = [A, B] = A\overline{B}\,\overline{A}B.$$

We can therefore reformulate (and, actually, easily reprove) some of the results of Section 5.2 in these algebraic terms. For example, Lemma 5.14 (heads exchange) translates to

$$AB = B[\overline{B}, \overline{A}]A,$$

and its variants given in Figure 22 to

$$AB = B\overline{[A, B]}A = BA[\overline{A}, B] = [A, \overline{B}]BA.$$

Lemma 5.17 (antisymmetry) also reformulates nicely; for example the "initial case" shown in Figure 25 can be restated as

$$[B, A] = \overline{[\overline{A}, \overline{B}]}.$$

Finally, Lemma 5.18 (fork) is simply

$$[\cdots[A, A]\cdots] = 1.$$

In the sequel, although we will still favor the more explicit diagrammatical language, we shall sometimes make use of this algebraic formalism.

6.2 The normalized Alexander polynomial for welded long knots

Let L be a welded long knot diagram. Suppose that the group of L has presentation $G(L) = \langle x_1, \ldots, x_m \mid r_1, \ldots, r_n \rangle$ for some m and n. Consider the $n \times m$ *Jacobian*

matrix $M = (\varphi(\partial r_i/\partial x_j))_{i,j}$, where $\partial/\partial x_j$ denotes the Fox free derivative in the variable x_j and where $\varphi\colon \mathbb{Z}F(x_1,\dots,x_m) \to \mathbb{Z}[t^{\pm 1}]$ is the ring homomorphism mapping each generator x_i of the free group $F(x_1,\dots,x_m)$ to t.

The *Alexander polynomial* of L, denoted by $\Delta_L(t) \in \mathbb{Z}[t^{\pm 1}]$, is defined as the greatest common divisor of the $(m-1)\times(m-1)$ minors of M, which is well defined up to a unit factor.

In order to remove the indeterminacy in the definition of $\Delta_L(t)$, we further require that $\Delta_L(1) = 1$ and that $d\Delta_L/dt(1) = 0$. The resulting invariant is the *normalized Alexander polynomial* of L, denoted by $\widetilde{\Delta}_L$ (see eg [14]). Taking the power series expansion at $t = 1$ as

$$\widetilde{\Delta}_L(t) = 1 + \sum_{k\geq 2} \alpha_k(L)(1-t)^k$$

thus defines an infinite sequence of integer-valued invariants α_k of welded long knots. (Our definition slightly differs from the one used in [14], by a factor $(-1)^k$.)

Definition 6.3 We call the invariant α_k the k^{th} *normalized coefficient* of the Alexander polynomial.

We now give a realization result for the coefficients α_k in terms of w–trees. Consider the welded long knots L_k or $\overline{L}_k$ $(k \geq 2)$ defined in Figure 31. We stress that, despite what the notation might suggest, these two welded long knots are not inverse of one another; however, this will be indeed the fact when working up to w_k–equivalence in Section 7.

Figure 31: The welded long knots L_k or $\overline{L}_k$ given by surgery along a single w_k–tree $(k \geq 2)$

Lemma 6.4 *Let $k \geq 2$. The normalized Alexander polynomials of L_k and $\overline{L}_k$ are given by*

$$\widetilde{\Delta}_{L_k}(t) = 1 + (1-t)^k \quad \text{and} \quad \widetilde{\Delta}_{\overline{L}_k}(t) = 1 - (1-t)^k.$$

Note that these are genuine equalities: there are no higher-order terms. In particular, we have $\alpha_i(L_k) = -\alpha_i(\overline{L}_k) = \delta_{ik}$.

Proof of Lemma 6.4 The presentation for $G(L_k)$ given by the defining w_k–tree presentation is $\langle l, r \mid R_k l R_k^{-1} r^{-1} \rangle$, where $R_k = \big[\big[\cdots\big[[l, r^{-1}], r^{-1}\big], r^{-1}\big]\cdots\big], r^{-1}\big]$ is a length k commutator. One can show inductively that

$$\varphi\left(\frac{\partial R_k}{\partial l}\right) = (1-t)^{k-1} \quad \text{and} \quad \varphi\left(\frac{\partial R_k}{\partial r}\right) = -(1-t)^{k-1},$$

so that the normalized Alexander polynomial is given by $\widetilde{\Delta}_{L_k}(t) = 1 + (1-t)^k$. The result for $\overline{L}_k$ is completely similar, and is left to the reader. □

The following might be well known; the proof is completely straightforward and is thus omitted.

Lemma 6.5 *The normalized Alexander polynomial of welded long knots is multiplicative.*

Lemma 6.5 implies the following additivity result:

Corollary 6.6 *Let k be a positive integer and let K be a welded long knot with $\alpha_i(K) = 0$ for $i \leq k-1$. Then $\alpha_k(K \cdot K') = \alpha_k(K) + \alpha_k(K')$ for any welded long knot K'.*

6.3 Welded Milnor invariants

We now recall the general virtual extension of Milnor invariants given in [1], which is an invariant of welded string links. This construction is intrinsically topological, since it is defined via the Tube map as the 4–dimensional analogue of Milnor invariants for (ribbon) knotted annuli in 4–space.

Given an n–component welded string link L, consider the group $G(L)$ defined in Section 6.1. Consider also the free groups F^l and F^u generated by the n "lower" and "upper" Wirtinger generators, ie the generators associated with the n arcs of L containing the initial or terminal points, respectively, of each component. Recall that the lower central series of a group G is the family of nested subgroups $\{\Gamma_k G\}_{k\geq 1}$ defined recursively by $\Gamma_1 G = G$ and $\Gamma_{k+1} G = [G, \Gamma_k G]$. Then, for each $k \geq 1$, we have a sequence of isomorphisms

$$F_n/\,\Gamma_k F_n \simeq F^l/\,\Gamma_k F^l \simeq G(L)/\,\Gamma_k G(L) \simeq F^u/\,\Gamma_k F^u \simeq F_n/\,\Gamma_k F_n,$$

where F_n is the free group on $m_1, \ldots, m_n$. This fact relies heavily on the topological realization of welded string links as ribbon knotted annuli in 4–space by the Tube

map. As noted in Remark 6.1, $G(L)$ is isomorphic to the fundamental group of the complement of the surface $\mathrm{Tube}(L)$ in 4–space, and the above sequence of isomorphism expresses, at the topological level, the "top" meridians of this complement, as conjugates of the "bottom" ones; see Section 5 of [1]. More precisely, the conjugating element is given, for each component of $\mathrm{Tube}(L)$, by the associated *preferred longitude*, as defined in [1, Remark 2.19]. For each $i \in \{1,\dots,n\}$ and each k, this defines a unique element $\lambda_i^k \in F_n/\Gamma_k F_n$, which we call the *combinatorial i^{th} longitude*. In this way, we associate to L an element $\varphi_k(L)$ of $\mathrm{Aut}(F_n/\Gamma_k F_n)$, which maps each generator m_i to its conjugate $\lambda_i^k m_i \overline{\lambda_i^k}$.

Now, consider the *Magnus expansion*, which is the group homomorphism $E\colon F_n \to \mathbb{Z}\langle\langle X_1,\dots,X_n\rangle\rangle$ mapping each generator m_i to the formal power series $1+X_i$.

Definition 6.7 For each sequence $I = i_1\cdots i_{m-1}i_m$ of (possibly repeating) indices in $\{1,\dots,n\}$, the *welded Milnor invariant* $\mu_I^w(L)$ of L is the coefficient of the monomial $X_{i_1}\cdots X_{i_{m-1}}$ in $E(\lambda_{i_m}^k)$ for any $k \geq m$. The number of indices in I is called the *length* of the invariant.

Note that welded Milnor invariants of length m do not depend on the choice of k above as soon as $k \geq m$.

For example, the simplest welded Milnor invariants μ_{ij}^w indexed by two distinct integers i and j are the so-called virtual linking numbers $\mathrm{lk}_{i/j}$ (see [9, Section 1.7]).

Remark 6.8 This is a welded extension of the classical Milnor μ–invariants, in the sense that if L is a (classical) string link, then $\mu_I(L) = \mu_I^w(L)$ for any sequence I.

The following realization result, in terms of w–trees, is to be compared with [24, page 190] and [33, Lemma 4.1].

Lemma 6.9 *Let $I = i_1\cdots i_k$ be a sequence of nonrepeated indices in $\{1,\dots,n\}$, and set $\sigma(I) = i_{\sigma(1)}\cdots i_{\sigma(k-2)}i_{k-1}i_k$ for any σ in the symmetric group S_{k-2} of degree $k-2$.*

Consider the w*–tree T_I for the trivial n–string link diagram $\mathbf{1}_n$ shown in Figure 32. Then we have*

$$\mu^w_{\sigma(I)}((\mathbf{1}_n)_{T_I}) = \begin{cases} 1 & \text{if } \sigma = \mathrm{id}, \\ 0 & \text{otherwise.} \end{cases}$$

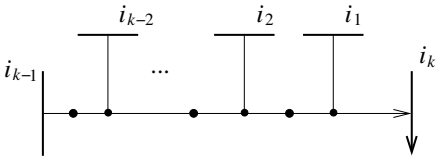

Figure 32: The w_{k-1}–tree $T_{i_1,i_2,\dots,i_{k-1},i_k}$ for $\mathbf{1}_n$

Moreover, for all $\sigma \in S_{k-2}$, we have

$$\mu^w_{\sigma(I)}((\mathbf{1}_n)_{T_I}) = -\mu^w_{\sigma(I)}((\mathbf{1}_n)_{\overline{T}_I}),$$

where $\overline{T}_I$ is the w*–tree obtained from T_I by inserting a twist in the terminal edge.*

Proof This is a straightforward calculation, based on the observation that the combinatorial $(i_k)^{\text{th}}$ longitude of T_I is given by

$$\lambda^k_{i_k} = [i_1, [i_2, \dots, [i_{k-3}, [i_{k-2}, i_{k-1}^{-1}]^{-1}]^{-1} \cdots]^{-1}]$$

(all other longitudes are clearly trivial). □

Remark 6.10 The above definition can be adapted to welded link invariants, which involves, as in the classical case, a recurring indeterminacy depending on lower-order invariants. In particular, the first nonvanishing invariants are well-defined integers, and Lemma 6.9 applies in this case.

Finally, let us add the following additivity result:

Lemma 6.11 *Let L and L' be two welded string links of the same number of components. Let m (resp. m') be the integer such that all welded Milnor invariants of L (resp. L') of length $\le m$ (resp. $\le m'$) are zero. Then $\mu^w_I(L \cdot L') = \mu^w_I(L) + \mu^w_I(L')$ for any sequence I of length $\le m + m'$.*

The proof is strictly the same as in the classical case, as for example in [22, Lemma 3.3], and is therefore left to the reader.

6.4 Finite-type invariants

The *virtualization move* is a local move on diagrams which replaces a classical crossing by a virtual one. We call the converse local move the *devirtualization* move.

Given a welded diagram L and a set C of classical crossings of L, we denote by L_C the welded diagram obtained by applying the virtualization move to all crossings in C; we also denote by $|C|$ the cardinality of C.

Definition 6.12 [9] An invariant v of welded knotted objects, taking values in an abelian group, is a *finite-type invariant of degree* $\leq k$ if, for any welded diagram L and any set S of $k+1$ classical crossings of L, we have

$$\sum_{S' \subset S} (-1)^{|S'|} v(L_{S'}) = 0. \tag{6-1}$$

An invariant is of degree k if it is of degree $\leq k$, but not of degree $\leq k-1$.

Remark 6.13 This definition is strictly similar to the usual notion of finite-type (or Goussarov–Vassiliev) invariants for classical knotted objects, with the virtualization move now playing the role of the crossing change. Since a crossing change can be realized by (de)virtualization moves, we have that the restriction of any welded finite-type invariant to classical objects is a Goussarov–Vassiliev invariant.

The following is shown in [14] (in the context of ribbon 2–knots; see Remark 6.1).

Lemma 6.14 *For each $k \geq 2$, the k^{th} normalized coefficient α_k of the Alexander polynomial is a finite-type invariant of degree k.*

It is known that classical Milnor invariants are of finite type [4; 21]. Using essentially the same arguments, it can be shown that, for each $k \geq 1$, length $k+1$ welded Milnor invariants of string links are finite-type invariants of degree k. The key point here is that a virtualization, just like a crossing change, corresponds to conjugating or not at the virtual knot group level. Since we will not make use of this fact in this paper, we will not provide a full and rigorous proof here. Indeed, formalizing the above very simple idea, as done by Bar-Natan in [4] in the classical case, turns out to be rather involved. Note, however, that we will use a consequence of this fact which, fortunately, can easily be proved directly; see Remark 7.6.

Remark 6.15 The Tube map recalled in Section 2.2 is also compatible with this finite-type invariant theory, in the following sense. Suppose that some invariant of welded knotted objects v extends naturally to an invariant $v^{(4)}$ of ribbon knotted objects, so that

$$v^{(4)}(\mathrm{Tube}(D)) = v(D),$$

for any diagram D. Note that this is the case for the virtual knot group, the normalized Alexander polynomial and welded Milnor invariants, essentially by Remark 6.1. Then,

if v is a degree k finite-type invariant, so is $v^{(4)}$, in the sense of the finite-type invariant theory of [14; 19]. Indeed, if two diagrams differ by a virtualization move, then their images by Tube differ by a "crossing changes at crossing circles", which is a local move that generates the finite-type filtration for ribbon knotted objects; see [19].

7 w_k–equivalence

We now define and study a family of equivalence relations on welded knotted objects, using w–trees. We explain the relation with finite-type invariants, and give several supplementary technical lemmas for w–trees.

7.1 Definitions

Definition 7.1 For each $k \geq 1$, the w_k–equivalence is the equivalence relation on welded knotted objects generated by generalized Reidemeister moves and surgery along w_l–trees for $l \geq k$. More precisely, two welded knotted objects W and W' are w_k–equivalent if there exists a finite sequence $\{W^i\}_{i=0}^n$ of welded knotted objects such that, for each $i \in \{1, \dots, n\}$, W^i is obtained from W^{i-1} either by a generalized Reidemeister move or by surgery along a w_l–tree for some $l \geq k$.

The w_k–equivalence becomes finer as the degree k increases, in the sense that the w_{k+1}–equivalence implies the w_k–equivalence.

The notion of w_k–equivalence is a bit subtle, in the sense that it involves moves both on diagrams and on w–tree presentations. Let us try to clarify this point by introducing the following:

Notation 7.2 Let (V, T) and (V, T') be two w–tree presentations of some diagrams, and let $k \geq 1$ be an integer. Then we use the notation

$$(V, T) \xrightarrow{k} (V, T')$$

if there is a union T'' of w–trees for V of degree $\geq k$ such that $(V, T) = (V, T' \cup T'')$.

Note that we have the implication

$$(V, T) \xrightarrow{k} (V, T') \implies V_T \overset{k}{\sim} V_{T'}.$$

Therefore, statements given in the terms of Notation 7.2 will be given when possible.

We do not know, however, whether the converse implication is true. In other words, we do not know whether a w_k–equivalence version of [13, Proposition 3.22] holds.

7.2 Cases $k = 1$ and 2

We now observe that w_1–moves and w_2–moves are equivalent to familiar local moves on diagrams.

We already saw in Figure 6 that surgery along a w–arrow is equivalent to a devirtualization move. Clearly, by the inverse move (5), this is also true for a virtualization move. It follows immediately that any two welded links or string links of the same number of components are w_1–equivalent.

Let us now turn to the w_2–equivalence relation. Recall that the right-hand side of Figure 2 depicts the *UC move*, which is the forbidden move in welded theory. We have:

Lemma 7.3 *A w_2–move is equivalent to a UC move.*

Proof Figure 33 shows that the UC move is realized by surgery along a w_2–tree. Note that, in the figure, we had to choose several local orientations on the strands; we leave it to the reader to check that the other cases of local orientations follow from the same argument, by simply inserting twists near the corresponding tails.

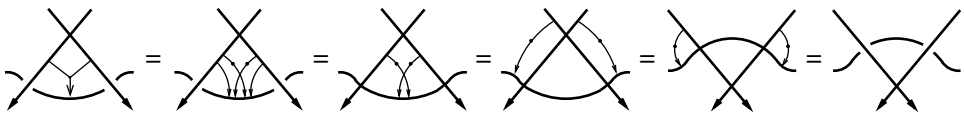

Figure 33: Surgery along a w_2–tree implies the UC move.

Conversely, Figure 34 shows that surgery along a w_2–tree is achieved by the UC move, hence that these two local moves are equivalent. □

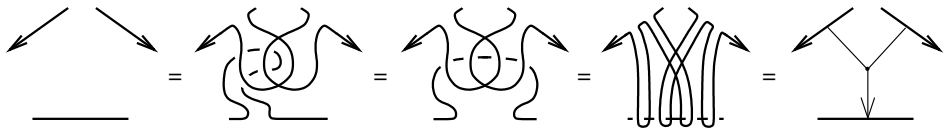

Figure 34: The UC move implies surgery along a w_2–tree.

It was shown in [2] that two welded (string) links are related by a sequence of UC moves, ie are w_2–equivalent, if and only if they have same welded Milnor invariants μ^w_{ij}. In particular, any two welded (long) knots are w_2–equivalent.

Remark 7.4 The fact that any two welded (long) knots are w_2–equivalent can also easily be checked directly using arrow calculus. Starting from an arrow presentation of a welded (long) knot, one can use the (tails, heads and head–tail) exchange move (3) and Lemmas 5.14 and 5.16 to separate and isolate all w–arrows, as in the figure of the isolated move (4), up to addition of higher-order w–trees. Each w–arrow is then equivalent to the empty one by move (4).

7.3 Relation to finite-type invariants

One of the main points in studying welded (and classical) knotted objects up to w_k–equivalence is the following:

Proposition 7.5 *Two welded knotted objects that are w_k–equivalent for some $k \geq 1$ cannot be distinguished by finite-type invariants of degree $< k$.*

Proof The proof is formally the same as Habiro's result relating C_n–equivalence (see Section 10.4) to Goussarov–Vassiliev finite-type invariants [13, Section 6.2], and is summarized below.

First, recall that, given a diagram L and k unions $W_1, \dots, W_k$ of w–arrows for L, the bracket $[L; W_1, \dots, W_k]$ stands for the formal linear combination of diagrams

$$[L; W_1, \dots, W_k] := \sum_{I \subset \{1,\dots,k\}} (-1)^{|I|} L_{\bigcup_{i \in I} W_i}.$$

Note that, if each W_i consists of a single w–arrow, then the defining equation (6-1) of finite-type invariants can be reformulated as the vanishing of (the natural linear extension of) a welded invariant on such a bracket. Note also that if, say, W_1 is a union of w–arrows $W_1^1, \dots, W_1^n$, then we have the equality

$$[L; W_1, W_2, \dots, W_k] = \sum_{j=1}^{n} [L_{W_1^1 \cup \dots \cup W_1^{j-1}}; W_1^j, W_2, \dots, W_k].$$

Hence, an invariant of degree $< k$ vanishes on $[L; W_1, \dots, W_k]$.

Now, suppose that T is a w_k–tree for some diagram L, and label the tails of T from 1 to k. Consider the expansion of T, and denote by W_i the union of all w–arrows running from (a neighborhood of) tail i to (a neighborhood of) the head of T. Then $L_T = L_{\bigcup_{i=1}^k W_i}$ and, according to the Brunnian-type property of w–trees noted in

Proposition 5.5, we have $L_{\bigcup_{i\in I} W_i} = L$ for any $I \subsetneq \{1,\dots,k\}$. Therefore, we have

$$L_T - L = (-1)^k [L; W_1, \dots, W_k],$$

which, according to the above observation, implies Proposition 7.5. □

We will show in Section 8 that the converse of Proposition 7.5 holds for welded knots and long knots.

Remark 7.6 It follows in particular from Proposition 7.5 that Milnor invariants of length $\leq k$ are invariants under w_k–equivalence. This can also be shown directly by noting that, if we perform surgery on a diagram L along some w_k–tree, this can only change elements of $G(L)$ by terms in $\Gamma_k F$.

7.4 Some technical lemmas

We now collect some supplementary technical lemmas, in terms of w_k–equivalence. The next result allows us to move twists across vertices.

Lemma 7.7 (twist) *Let $k \geq 2$. The following holds for a w_k–tree:*

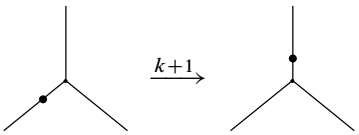

Note that this move implies the converse one, by using Lemma 5.17 (antisymmetry) and the twist involutivity.

Proof Denote by n the number of edges of T in the unique path connecting the trivalent vertex shown in the statement to the head. Note that $1 \leq n \leq k-1$. We will prove by induction on d the following claim, which is a stronger form of the desired statement:

Claim 7.8 *For all $k \geq 2$, and for any w_k–tree T, the following equality holds, where S is a union of w–trees of degree $> k$* (using the same graphical convention as in Convention 5.10)*:*

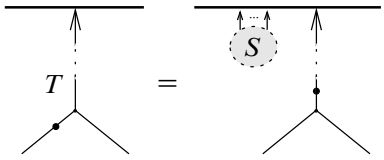

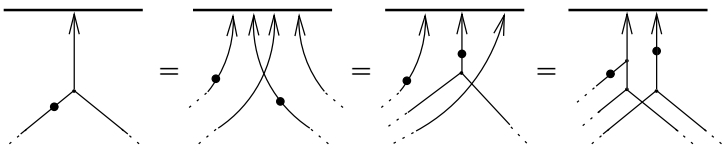

Figure 35: Proof of the twist lemma, case $n = 1$

The case $n = 1$ of the claim is given in Figure 35. There, the first equality uses (E) and the second equality follows from Lemma 5.14 (heads exchange) — actually, from Remark 5.15 — applied at the two rightmost heads, and Lemma 5.9 (inverse). The third equality also follows from Remark 5.15 and the inverse lemma. Note that this can equivalently be shown using the algebraic formalism of Section 6.1.2; more precisely, the above figure translates to the simple equalities

$$[\bar{A}, B] = \bar{A}\bar{B}AB = \overline{A[A, B]}A = [\bar{A}, [A, B]]\overline{[A, B]}.$$

Observe that, in this algebraic setting, $d = n - 1$ is the *depth* of $[\bar{A}, B]$ in an iterated commutator $[\cdots, [\bar{A}, B]\cdots] \in \Gamma_m F$. For the inductive step, consider an element $\big[C, [\cdots, [\bar{A}, B]\cdots]\big] \in \Gamma_k F$, where $C \in \Gamma_l F$ and $[\cdots, [\bar{A}, B]\cdots] \in \Gamma_m F$ for some integers l and m such that $l + m = k$. Observe also that the induction hypothesis gives the existence of some $S \in \Gamma_{m+1} F$ such that

$$[\cdots, [\bar{A}, B]\cdots] = S[\cdots, \overline{[A, B]}\cdots],$$

and hence

$$\overline{[\cdots, [\bar{A}, B]\cdots]} = \overline{[\cdots, \overline{[A, B]}\cdots]}\bar{S}.$$

The inductive step is then given by

$$\begin{aligned}
&\big[C, [\cdots, [\bar{A}, B]\cdots]\big] \\
&\quad = C\overline{[\cdots, [\bar{A}, B]\cdots]}\bar{C}[\cdots, [\bar{A}, B]\cdots] \\
&\quad = C\overline{[\cdots, \overline{[A, B]}\cdots]}\bar{S}\bar{C}S[\cdots, \overline{[A, B]}\cdots] \quad \text{(induction hypothesis)} \\
&\quad = GC\overline{[\cdots, \overline{[A, B]}\cdots]}\bar{C}[\cdots, \overline{[A, B]}\cdots] \quad \text{(Lemma 5.14, heads exchange)} \\
&\quad = G\big[C, [\cdots, \overline{[A, B]}\cdots]\big],
\end{aligned}$$

where G is some term in $\Gamma_{k+1} F$. (The reader is invited to draw the corresponding diagrammatic argument.) □

Remark 7.9 By a symmetric argument, we can prove a variant of Claim 7.8 where the heads of S are to the right-hand side of the w–tree in the figure.

Next, we address the move exchanging a head and a tail of two w–trees of arbitrary degree.

Lemma 7.10 *The following holds:*

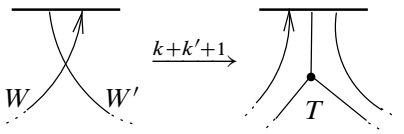

Here, W and W' are a w_k–tree and a $\mathrm{w}_{k'}$–tree, respectively, for some $k, k' \geq 1$, and T is a $\mathrm{w}_{k+k'}$–tree as shown.

Proof Consider the path of edges of W' connecting the tail shown in the figure to the head, and denote by n the number of edges in this path; we have $1 \leq n \leq k'$. The proof is by induction on n. More precisely, we prove by induction on n the following stronger statement:

Claim 7.11 *Let $k, k' \geq 2$. Let W, W' and T be as above. The following equality holds, where S denotes a union of* w*–trees of degree $> k + k'$:*

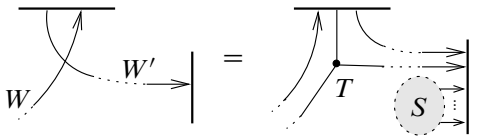

The case $n = 1$ of the claim is a consequence of Lemma 5.16 (head–tail exchange), Claim 7.8 and the involutivity of twists. The proof of the inductive step is illustrated in Figure 36. The first equality in Figure 36 is an application of (E) to the $\mathrm{w}_{k'}$–tree W', while the second equality uses the induction hypothesis. The third (vertical) equality then follows from recursive applications of Lemma 5.14 (heads exchange), and uses also Convention 5.10. Further heads exchanges give the fourth equality, and the final one is given by (E). □

Remark 7.12 We have the following variation of Claim 7.11, which we implicitly used in the above proof (the second equality):

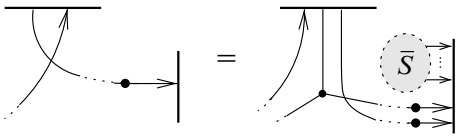

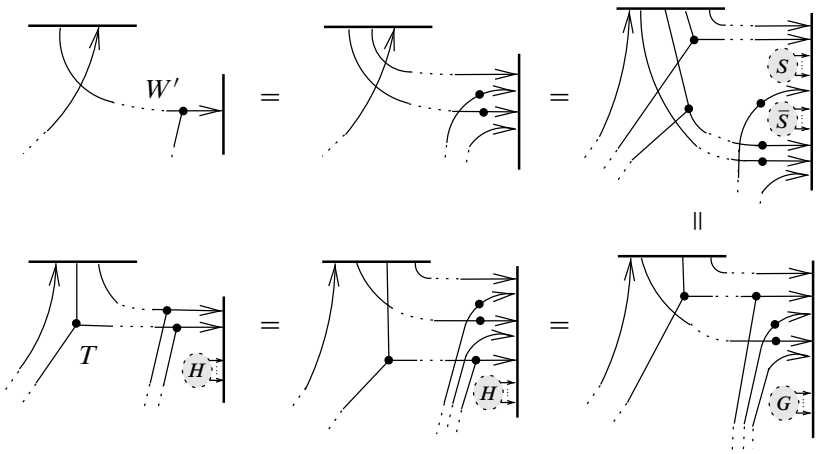

Figure 36: Here, S (resp. G and H) represents a union of w–trees of degree $> k+k'$ (resp. degree $> k+k'+1$).

We leave it as an exercise to the reader to check that it actually follows from Claim 7.11, using Lemma 5.9 (inverse) and Convention 5.10.

We note the following consequence of Lemma 5.14 and Claim 7.11:

Corollary 7.13 *Let T and T' be two* w*–trees, of degrees k and k'. We can exchange the relative position of two adjacent endpoints of T and T', at the expense of additional* w*–trees of degree $\geq k+k'$.*

Proof There are three types of moves to be considered. First, exchanging two tails can be freely performed by the tails exchange move (3). Second, it follows from Lemma 5.14 (heads exchange) that exchanging the heads of these two w–trees can be performed at the cost of one $\mathrm{w}_{k+k'}$–tree. Third, by Claim 7.11, exchanging a tail of one of these w–trees and the head of the other can be achieved up to addition of w–trees of degree $\geq k+k'$. □

Remark 7.14 Let F be a union of w–trees of degree $\geq k$ with adjacent heads. Then the (proof of the) above result implies more precisely that:

- The heads of F can be exchanged with a bunch of heads of w–trees of degree $\geq k'$, at the cost of degree $\geq k+k'$ w–trees which can be located on either side of the commuting bunches.

- The heads of F can be exchanged with the tail of a $\mathrm{w}_{k'}$–tree T, at the cost of degree $\geq k+k'$ w–trees whose heads are located on either side of the head of T.

Let us also note, for future use, the following consequence of these exchange results. We denote by $\mathbf{1}_n$ the trivial n–component string link diagram.

Lemma 7.15 *Let k and l be integers such that $k \geq l \geq 1$. Let W be a union of* w*–trees for $\mathbf{1}_n$ of degree $\geq l$. Then*

$$(\mathbf{1}_n)_W \overset{k+1}{\sim} (\mathbf{1}_n)_{T_1} \cdots (\mathbf{1}_n)_{T_m} \cdot (\mathbf{1}_n)_{W'},$$

where $T_1, \dots, T_m$ are w_l–trees and W' is a union of w*–trees of degree in $\{l+1, \dots, k\}$.*

Proof This is shown by repeated applications of Corollary 7.13. More precisely, we use exchange moves to rearrange the w_l–trees $T_1, \dots, T_m$ in W so that they sit in disjoint disks D_i for $i = 1, \dots, m$, which intersect each component of $\mathbf{1}_n$ at a single trivial arc, so that $(\mathbf{1}_n)_{\bigcup_i T_i} = (\mathbf{1}_n)_{T_1} \cdots (\mathbf{1}_n)_{T_m}$. By Corollary 7.13, this is achieved at the expense of w–trees of degree $\geq l+1$, which may intersect those disks. But further exchange moves allow us to move all higher-degree w–trees *under* $\bigcup_i D_i$, according to the orientation of $\mathbf{1}_n$, now at the cost of additional w–trees of degree $\geq l+2$, which possibly intersect $\bigcup_i D_i$. We can repeat this procedure until the only higher-degree w–trees intersecting $\bigcup_i D_i$ have degree $> k$, which gives the desired equivalence. □

Finally, we give a w–tree version of the IHX relation.

Lemma 7.16 (IHX) *The relation of Figure 37 holds.*

There, I, H and X are three w_k–trees for some $k \geq 3$.

Proof We prove this lemma using the algebraic formalism of Section 6.1.2, for simplicity. We prove the following stronger version:

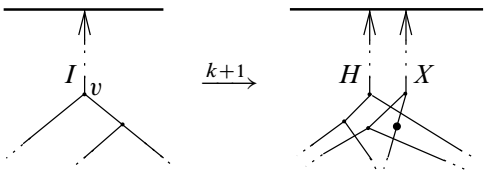

Figure 37: The IHX relation for w–trees

Claim 7.17 *For all $k \geq 2$, we have*

$$\underbrace{\big[\cdots,[A,[B,C]]\cdots\big]}_{\in \Gamma_k F} = S\big[\cdots,[[A,B],C]\cdots\big]\big[\cdots,[[A,C],\overline{B}]\cdots\big]$$

for some $S \in \Gamma_{k+1}F$.

The proof is by induction on the depth d of $[A,[B,C]]$ in the iterated commutator $[\cdots,[A,[B,C]]\cdots]$, as defined in the proof of Claim 7.8. Recall that, diagrammatically, the depth of $[A,[B,C]]$ is the number of edges connecting the vertex v in Figure 37 to the head. The case $d=0$ is given by

$$\begin{aligned}
[A,[B,C]] &= A\overline{C}BC\,\overline{B}\,\overline{A}B\overline{C}\,\overline{B}C \\
&= A\overline{C}BC\,\overline{A}[A,B]\overline{C}\,\overline{B}C \\
&= A\overline{C}BC\,\overline{A}[[A,B],C]\overline{C}[A,B]\overline{B}C \\
&= R'[[A,B],C]A\overline{C}BC\,\overline{A}\overline{C}[A,B]\overline{B}C && \text{(Lemma 5.14, heads exchange)} \\
&= R'[[A,B],C]A\overline{C}BC\,\overline{A}\overline{C}A\,\overline{B}\,\overline{A}C \\
&= R'[[A,B],C]A\overline{C}B[C,A]\overline{B}\,\overline{A}C \\
&= R'[[A,B],C]A\overline{C}[C,A][[\overline{A},\overline{C}],\overline{B}]\overline{A}C \\
&= R[[A,B],C][[\overline{A},\overline{C}],\overline{B}] && \text{(Lemma 5.14, heads exchange)} \\
&= R[[A,B],C]S'[[A,C],\overline{B}] && \text{(Lemma 7.7, twist)} \\
&= S[[A,B],C][[A,C],\overline{B}] && \text{(Lemma 5.14, heads exchange),}
\end{aligned}$$

where R, R', S' and S are some elements of $\Gamma_{k+1}F$.

For the inductive step, let $I' = [\cdots,[A,[B,C]]\cdots]$ be an element of $\Gamma_m F$, for some $m \geq 3$, such that $[A,[B,C]]$ has depth d, and set $H' = [\cdots,[[A,B],C]\cdots]$ and $X' = [\cdots,[[A,C],\overline{B}]\cdots]$. By the induction hypothesis, there exists an element $S \in \Gamma_{m+1}$ such that $I' = SH'X'$. Let $D \in \Gamma_l F$ such that $l+m=k$. Then we have

$$\begin{aligned}
[D,I'] = D\overline{I'}\,\overline{D}I' &= D\overline{X'}\,\overline{H'}\,\overline{S}\,\overline{D}SH'X' && \text{(induction hypothesis)} \\
&= R'D\overline{X'}\,\overline{H'}\,\overline{D}H'X' && \text{(Lemma 5.14, heads exchange)} \\
&= R'D\overline{X'}\,\overline{D}[D,H']X' \\
&= R[D,H']D\overline{X'}\,\overline{D}X' && \text{(Lemma 5.14, heads exchange)} \\
&= R[D,H'][D,X'],
\end{aligned}$$

where R and R' are some elements in $\Gamma_{k+1}F$. □

8 Finite-type invariants of welded knots and long knots

We now use the w_k–equivalence relation to characterize finite-type invariants of welded (long) knots. Topological applications for surfaces in 4–space are also given.

8.1 w_k–equivalence for welded knots

The fact, noted in Section 7.2, that any two welded knots are w_i–equivalent for $i = 1, 2$, generalizes widely, as follows:

Theorem 8.1 *Any two welded knots are w_k–equivalent for any $k \geq 1$.*

An immediate consequence is the following:

Corollary 8.2 *There is no nontrivial finite-type invariant of welded knots.*

This was already noted for rational-valued finite-type invariants by Bar-Natan and Dancso [5]. Also, we have the following topological consequence, which we prove in Section 10.2:

Corollary 8.3 *There is no nontrivial finite-type invariant of ribbon torus knots.*

Theorem 8.1 is a consequence of the following, stronger statement:

Lemma 8.4 *Let k and l be integers such that $k \geq l \geq 1$, and let W be a union of w–trees for O. There is a union W_l of w–trees of degree $\geq l$ such that $O_W \overset{k+1}{\sim} O_{W_l}$.*

Proof The proof is by induction on l. The initial case, ie $l = 1$ for any fixed integer $k \geq 1$, is obvious. Assume that W is a union of w–trees of degree $\geq l$, and pick a w_l–tree $T \in W$. Let us call "external" any vertex of a w–tree that is connected to two tails; note that a w–tree always contains at least one external vertex. So, consider an external vertex in T, and the two tails connected to it. If the two tails are adjacent on O then, possibly after using Lemma 5.17 (antisymmetry), we can use Lemma 5.18 (fork) to delete T; otherwise, we use Corollary 7.13 repeatedly until these two tails become adjacent. Since all the moves performed in this procedure are achieved at the cost of w–trees of degree $> l$, we can iterate this process and conclude that T can be deleted up to w_{k+1}–equivalence. This completes the proof. □

8.2 w_k–equivalence for welded long knots

We now turn to the case of long knots. In what follows, we use the notation $\mathbf{1}$ for the trivial long knot diagram (with no crossing).

As recalled in Section 7.2, it is known that any two welded long knots are w_i–equivalent for $i = 1, 2$. The main result of this section is the following generalization:

Theorem 8.5 *For each $k \geq 1$, welded long knots are classified up to w_k–equivalence by the normalized coefficients $\{\alpha_i\}_{2 \leq i < k}$ of the Alexander polynomial.*

Since the normalized coefficients of the Alexander polynomial are of finite type (Lemma 6.14), we obtain the following, which in particular gives the converse to Proposition 7.5 for welded long knots:

Corollary 8.6 *The following assertions are equivalent for any integer $k \geq 1$:*

- *Two welded long knots are w_k–equivalent.*
- *Two welded long knots share all finite-type invariants of degree $< k$.*
- *Two welded long knots have the same invariants $\{\alpha_i\}$ for $i < k$.*

Theorem 8.5 also implies the following, which was first shown by Habiro and Shima [16], and which will be proved in Section 10.2:

Corollary 8.7 *Finite-type invariants of ribbon 2–knots are determined by the (normalized) Alexander polynomial.*

Actually, we also recover a topological characterization of finite-type invariants of ribbon 2–knots due to Watanabe; see Section 10.2.

Moreover, by the multiplicative property of the normalized Alexander polynomial (Lemma 6.5), we have the following consequence:

Corollary 8.8 *Welded long knots up to w_k–equivalence form a finitely generated free abelian group for any $k \geq 1$.*

The proof of Theorem 8.5 uses the next technical lemma, which refers to the welded long knots L_k or $\overline{L}_k$ defined in Figure 31. As noted there, we have that $L_k \cdot \overline{L}_k$ is w_k–equivalent to the trivial string link, so it makes sense to set the notation $L_k^{-1} := \overline{L}_k$.

Lemma 8.9 *Let k and l be integers such that $k \geq l \geq 2$, and let W be a union of* w*–trees of degree $\geq l$ for $\mathbf{1}$. Then*

$$\mathbf{1}_W \overset{k+1}{\sim} (L_l)^x \cdot \mathbf{1}_{W'}$$

for some $x \in \mathbb{Z}$, where W' is a union of w*–trees of degree $\geq l + 1$.*

Proof of Theorem 8.5 assuming Lemma 8.9 We prove that, for any k and l such that $k \geq l \geq 1$, a welded long knot K satisfies

$$K \overset{k+1}{\sim} \left(\prod_{i=2}^{l-1} L_i^{x_i(K)} \right) \cdot \mathbf{1}_{W_l}, \tag{8-1}$$

where $(\mathbf{1}, W_l) \xrightarrow{l} (\mathbf{1}, \varnothing)$, and where

$$x_i(K) = \begin{cases} \alpha_i(K) & \text{if } i = 2, \\ \alpha_i(K) - \alpha_i\left(\prod_{j=2}^{i-1} L_j^{x_j(K)}\right) & \text{if } i > 2. \end{cases}$$

We proceed by induction on l. The cases $l = 1$ and 2 are clear, since any two welded long knots are w_2–equivalent, as observed in Section 7.2. Assume (8-1) for some $l \geq 2$ and any fixed $k \geq l$. By applying Lemma 8.9 to the welded long knot $\mathbf{1}_{W_l}$, we have $\mathbf{1}_{W_l} \overset{k+1}{\sim} (L_l)^x \cdot \mathbf{1}_{W_{l+1}}$, where $(\mathbf{1}, W_{l+1}) \xrightarrow{l+1} (\mathbf{1}, \varnothing)$. Using the additivity (Corollary 6.6) and finite-type (Lemma 6.14 and Proposition 7.5) properties of the normalized coefficients of the Alexander polynomial, we obtain that $x = x_l(K)$, thus completing the proof. □

Proof of Lemma 8.9 By Lemma 7.15, we may assume that

$$1_W \overset{k+1}{\sim} \mathbf{1}_{T_1} \cdots \mathbf{1}_{T_m} \cdot \mathbf{1}_{W'},$$

where each T_i is a single w_l–tree and W' is a union of w–trees of degree in $\{l+1, \ldots, k\}$.

Consider such a w_l–tree T_i. As in the proof of Lemma 8.4, we call "external" any vertex of T_i which is connected to two tails. In general, T_i might contain several external vertices, but by Lemma 7.16 (IHX) and Corollary 7.13, we can freely assume that T_i has only one external vertex, up to w_{k+1}–equivalence.

By Lemma 5.18 (fork) and the tails exchange move (3), if the two tails connected to this vertex are not separated by the head, then T_i is equivalent to the empty w–tree. Otherwise, using the tails exchange move, we can assume that these two tails are at the leftmost and rightmost positions among all endpoints of T_i along $\mathbf{1}$, as for example for the w_l–tree shown in Figure 38.

The result then follows from the observation shown in this figure.[6] Indeed, combining these equalities with the involutivity of twists and Lemma 7.7 (twist), we have that T_i

[6]The symmetric version of this observation, with one tail to the left of the shaded region and two to the right, follows from this one, by using head and tail reversal moves, together with Lemmas 5.17 (antisymmetry) and 7.7 (twist).

can be deformed, up to w_{k+1}–equivalence, into one of the two w_l–trees of Figure 31, at the cost of adding a union of w–trees of degree in $\{l+1,\dots,k\}$.

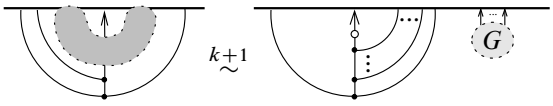

Figure 38: The shaded part contains all unrepresented edges of the w_l–tree, and G is a union of w–trees of degree in $\{l+1,\dots,k\}$.

Let us prove the equivalence of Figure 38. To this end, consider the union $A \cup F$ of a w–arrow A and a w_{l-1}–tree F as shown in Figure 39, left. On one hand, by Lemma 5.18 (fork), followed by the isolated move (4), we have that $\mathbf{1}_{A\cup F} = \mathbf{1}$.

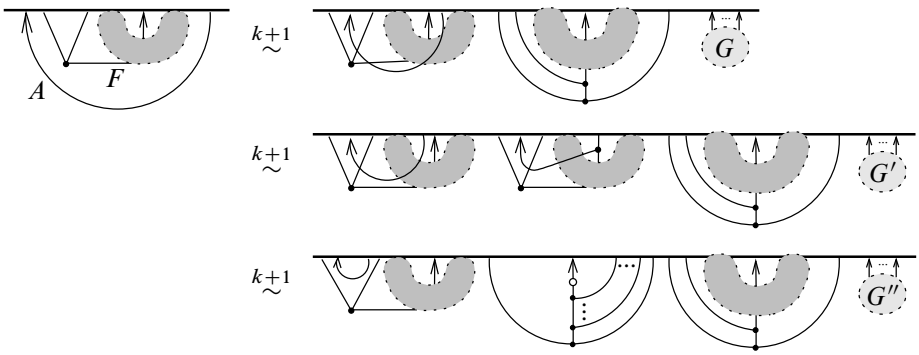

Figure 39: Here, G, G' and G'' are unions of w–trees of degree in $\{l+1,\dots,k\}$.

On the other hand, we can use Lemma 7.10 (head–tail exchange) to move the head of A across the adjacent tail of F, and apply the tails exchange move (3) to move the tail of A towards the head of F, thus producing, by Lemma 7.15, the first equivalence of Figure 39.[7] We can then apply the head–tail exchange lemma to move the tail of A across the head of F, which by Lemma 7.15 yields the second equivalence. Further applications of Lemma 7.15, together with Lemmas 5.17 (antisymmetry) and 7.7 (twist), give the third equivalence. Finally, the first term in the right-hand side of this equivalence is trivial by the isolated move (4) and the fork lemma. The equivalence of Figure 38 is then easily deduced, using the inverse lemmas, Lemmas 5.9 and 7.15. □

[7] To be more precise, these exchange moves produce w–tress of degree $> l$, which are pushed successively towards the right to G at the cost of degree $> k$ trees. The same comment holds for the other equivalences of Figure 39.

9 Homotopy arrow calculus

The previous section shows how the study of welded knotted objects of one component is well understood when working up to w_k–equivalence. The case of several components (welded links and string links), though maybe not out of reach, is significantly more involved.

One intermediate step towards a complete understanding of knotted objects of several components is to study these objects "modulo knot theory". In the context of classical (string) links, this leads to the notion of *link-homotopy*, where each individual component is allowed to cross itself; this notion was first introduced by Milnor [24], and culminated with the work of Habegger and Lin [11], who used Milnor invariants to classify string links up to link-homotopy. In the welded context, the analogue of this relation is generated by the *self-virtualization move*, where a crossing involving two strands of the same component can be replaced by a virtual one. In what follows, we simply call *homotopy* this equivalence relation on welded knotted objects, which we denote by $\overset{h}{\sim}$. This is indeed a generalization of link-homotopy, since a crossing change between two strands of the same component can be generated by two self-(de)virtualizations.

We have the following natural generalization of [25, Theorem 8]:

Lemma 9.1 *If I is a sequence of nonrepeated indices, then μ^w_I is invariant under homotopy.*

Proof The proof is essentially the same as in the classical case. Set $I = i_1 \cdots i_m$, with $i_j \neq i_k$ if $j \neq k$. It suffices to show that μ^w_I remains unchanged when a self-(de)virtualization move is performed on the i^{th} component, which is done by distinguishing two cases. If $i = i_m$, then the effect of this move on the combinatorial $(i_m)^{\text{th}}$ longitude is multiplication by an element of the normal subgroup N_i generated by m_i; each (nontrivial) term in the Magnus expansion of such an element necessarily contains X_{i_m} at least once, and thus μ^w_I remains unchanged. If $i \neq i_m$, then this move can only affect the combinatorial $(i_m)^{\text{th}}$ longitude by multiplication by an element of $[N_i, N_i]$: any nontrivial term in the Magnus expansion of such an element necessarily contains X_i at least twice. □

9.1 w–tree moves up to homotopy

Clearly, the w–arrow incarnation of a self-virtualization move is the deletion of a w–arrow whose tail and head are attached to the same component. In what follows, we

will call such a w–arrow a *self-arrow*. More generally, a *repeated* w–tree is a w–tree having two endpoints attached to the same component of a diagram.

Lemma 9.2 *Surgery along a repeated* w*–tree does not change the homotopy class of a diagram.*

Proof Let T be a w–tree having two endpoints attached to the same component. We must distinguish between two cases, depending on whether these two endpoints contain the head of T or not.

Case 1 (the head and some tail t of T are attached to the same component) Then we can simply expand T; the result contains a bunch of self-arrows, joining (a neighborhood of) t to (a neighborhood of) the head of T. By the Brunnian-type property of w–trees (Proposition 5.5), deleting all these self-arrows yields a union of w–arrows which is equivalent to the empty one.

Case 2 (two tails t_1 and t_2 of T are attached to the same component) Consider the path of edges connecting these two tails, and denote by n the number of edges connecting this path to the head; we proceed by induction on n. The case $n = 1$ is illustrated in Figure 40. As the first equality shows, one application of (E) yields four w–trees T_1, $\overline{T}_1$, T_2 and $\overline{T}_2$.

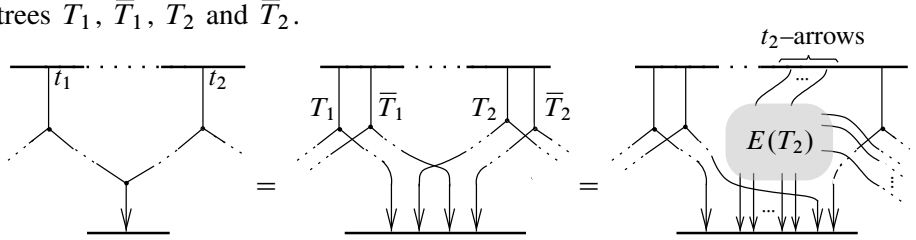

Figure 40: Proof of Lemma 9.2

For the second equality, expand the w–tree T_2, and denote by $E(T_2)$ the result of this expansion. Let us call "t_2–arrows" the w–arrows in $E(T_2)$ whose tail lie in a neighborhood of t_2. We can successively slide all other w–arrows in $E(T_2)$ along the t_2–arrows, and next slide the two w–trees T_1 and $\overline{T}_1$, using Remark 5.12; the result is a pair of repeated w–trees as in Case 1 above, which we can delete up to homotopy. Reversing the slide and expansion process in $E(T_2)$, we then recover $T_2 \cup \overline{T}_2$, which can be deleted by Lemma 5.9 (inverse). The inductive step is clear, using (E) and Lemma 5.9. □

Thanks to the previous result, the lemmas given in Section 7.4 for w–tree presentations still hold when working up to homotopy. More precisely, we have the following:

Lemma 9.3 *The following relations hold up to homotopy among* w*–trees:*

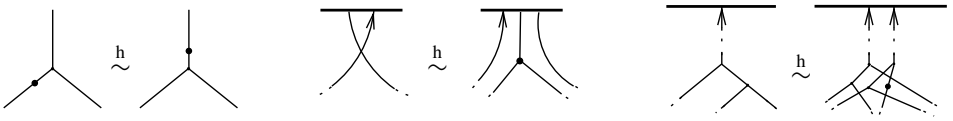

Proof This is a direct consequence of Lemma 9.2 and Lemmas 7.7, 7.10 and 7.16, respectively, since all w–trees realizing the equivalences in the latter statements are necessarily repeated. For example, in the statement of Lemma 7.7, all w_{k+1}–trees appearing from the w_{k+1}–equivalence have $k+2$ ends on at most $k+1$ strands and are thus repeated, which by Lemma 9.2 implies the first equivalence of the lemma. □

9.2 Homotopy classification of welded string links

Let $n \geq 2$. For each integer $i \in \{1,\dots,n\}$, denote by $\mathcal{S}_l(i)$ the set of all sequences $i_1 \cdots i_l$ of l distinct integers from $\{1,\dots,n\} \setminus \{i\}$ such that $i_j < i_l$ for all $j = 1,\dots,l-1$. Note that the lexicographic order endows the set $\mathcal{S}_l(i)$ with a total order.

For any sequence $I = i_1 \cdots i_{k-1} \in \mathcal{S}_{k-1}(i)$, consider the w_{k-1}–trees T_{Ii} and $\overline{T}_{Ii}$ for the trivial diagram $\mathbf{1}_n$ introduced in Lemma 6.9. Set

$$W_{Ii} := (\mathbf{1}_n)_{T_{Ii}} \quad \text{and} \quad W_{Ii}^{-1} := (\mathbf{1}_n)_{\overline{T}_{Ii}}.$$

We prove the following (compare with Theorem 4.3 of [33]). This gives a complete list of representatives for welded string links up to homotopy.

Theorem 9.4 *Let L be an n–component welded string link. Then L is homotopic to $l_1 \cdots l_{n-1}$, where, for each k,*

$$l_k = \prod_{i=1}^{n} \prod_{I \in \mathcal{S}_k(i)} (W_{Ii})^{x_I},$$

with

$$x_I = \begin{cases} \mu^w_{ji}(L) & \text{if } k = 1 \text{ and } I = j, \\ \mu^w_{Ii}(L) - \mu^w_{Ii}(l_1 \cdots l_{k-1}) & \text{if } k > 1. \end{cases}$$

As a consequence, we recover the following classification results:

Corollary 9.5 *Welded string links are classified up to homotopy by welded Milnor invariants indexed by nonrepeated sequences.*

Corollary 9.5 was first shown by Audoux, Bellingeri, Wagner and the first author [1]; their proof consists in defining a global map from welded string links up to homotopy to conjugating automorphisms of the reduced free group, then to use Gauss diagram to build an inverse map.

Remark 9.6 Corollary 9.5 is a generalization of the link-homotopy classification of string links by Habegger and Lin [11]; it is, indeed, shown in [1] that string links up to link-homotopy embed in welded string links up to homotopy. However, Theorem 9.4 does not allow us to recover the result of [11]. By Remark 6.8, it only implies that two classical string link diagrams are related by a sequence of isotopies and self-(de)virtualizations if and only if they have same Milnor invariants.

Proof of Theorem 9.4 Let L be an n–component welded string link. Pick an arrow presentation for L. By Lemma 7.15, we can freely rearrange the w–arrows up to w_n–equivalence, so that

$$L \overset{n}{\sim} \prod_{j\neq i} (W_{ji})^{x_{ji}} \cdot (\mathbf{1}_n)_{R_1} \cdot (\mathbf{1}_n)_{S_{\geq 2}}$$

for some integers x_{ji}, where R_1 is a union of self-arrows and $S_{\geq 2}$ is a union of w–trees of degree in $\{2,\dots,n-1\}$. Up to homotopy, we can freely delete all self-arrows, and using the properties of Milnor invariants (Lemmas 6.11 and 6.9, Remark 7.6 and Lemma 9.1), we have that $x_{ji} = \mu^w_{ji}(L)$ for all $j \neq i$. Hence, we have

$$L \overset{\mathrm{h}}{\sim} l_1 \cdot (\mathbf{1}_n)_{S_{\geq 2}}.$$

Next, we can separate, by a similar procedure, all w_2–trees in $S_{\geq 2}$. Repeated w_2–trees can be deleted thanks to Lemma 9.2. Next, we need the following general fact,[8] which is easily checked using Lemmas 5.17 (antisymmetry), 7.16 (IHX) and 7.7 (twist).

Claim 9.7 *Let T be a nonrepeated w_k–tree for $\mathbf{1}_n$, with $k \geq 2$, such that the head of T is attached to the i^{th} strand of $\mathbf{1}_n$. Then*

$$(\mathbf{1}_n)_T \overset{\mathrm{h}}{\sim} \prod_{i=1}^{N} (\mathbf{1}_n)_{T_i}$$

for some $N \geq 1$, where each T_i is a copy of either T_{Ii} or $\overline{T}_{Ii}$ for some $I \in \mathcal{S}_{k-2}(i)$.

[8] This is merely a w–tree version of the well-known fact that any Jacobi tree diagram can be written, up to antisymmetry and IHX, as a linear sum of "linear" tree diagrams; see eg [15, Figure 3].

Hence, we obtain

$$L \overset{\mathrm{h}}{\sim} l_1 \cdot \prod_{i=1}^{n} \prod_{I \in \mathcal{S}_2(i)} (W_{Ii})^{x_I} \cdot (\mathbf{1}_n)_{S_{\geq 3}}$$

for some integers x_I, where $S_{\geq 3}$ is a union of w–trees of degree in $\{3, \dots, n-1\}$. By using the properties of Milnor invariants, we have

$$\begin{aligned} \mu^w_{Ii}(L) &= \mu^w_{Ii}\Big(l_1 \cdot \prod_{i=1}^{n} \prod_{I \in \mathcal{S}_2(i)} (W_{Ii})^{x_I} \Big) \\ &= \mu^w_{Ii}(l_1) + \sum_{i=1}^{n} \sum_{I \in \mathcal{S}_2(i)} x_I \mu^w_{Ii}(W_{Ii}) \\ &= \mu^w_{Ii}(l_1) + x_I, \end{aligned}$$

thus showing that

$$L \overset{\mathrm{h}}{\sim} l_1 \cdot l_2 \cdot (\mathbf{1}_n)_{S_{\geq 3}}.$$

Iterating this procedure, using Claim 9.7 and the same properties of Milnor invariants, we eventually obtain that $L \overset{n}{\sim} l_1 \cdots l_{n-1}$. The result follows by Lemma 9.2, since w–trees of degree $\geq n$ for $\mathbf{1}_n$ are necessarily repeated. □

Remark 9.8 It was shown in [1] that Corollary 9.5, together with the Tube map, gives homotopy classifications of ribbon tubes and ribbon torus links (see Section 2.2). Actually, we can deduce easily a homotopy classification of ribbon string links in codimension 2, in any dimension; see [3].

10 Concluding remarks and questions

10.1 Welded arcs

There is yet another class of welded knotted object that we should mention here. A *welded arc* is an immersed oriented arc in the plane, up to generalized Reidemeister moves, OC moves and the additional move of Figure 41, left; see [18]. There, we represent the arc endpoints by large dots. We emphasize that these large dots are "free" in the sense that they can be freely isotoped in the plane. It can be checked that welded arcs have a well-defined composition rule, given by gluing two arc endpoints, respecting the orientations. This is actually a very natural notion from the 4–dimensional point of view; see Section 10.2 below.

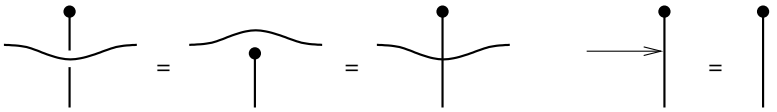

Figure 41: Additional moves for welded arcs and the corresponding extra w–tree move

Figure 41 also gives the additional move for welded arcs in terms of w–trees: we can freely delete a w–tree whose head is adjacent to an arc endpoint.

Observe that the proof of Lemma 8.9 applies verbatim to these objects, since it relies on an explicit sequence of local operations which holds for welded arcs. Furthermore, it is well known that the normalized Alexander coefficients are well defined for welded arcs, and that both Lemma 6.14 and Proposition 7.5 still hold for welded arcs; see eg [18, Section 3]. Hence, any α_i with $i < k$ is an invariant of w_k–equivalence.

This observation having been made, one shows that, for each $k \geq 1$, welded arcs are classified up to w_k–equivalence by the normalized coefficients $\{\alpha_i\}_{2 \leq i < k}$, by strictly following the proof of Theorem 8.5. This shows that welded arcs up to w_k–equivalence form an abelian group, which is isomorphic to that of welded long knots up to w_k–equivalence, for any $k \geq 1$.

To be more precise, there is a natural *capping* map C from welded long knots to welded arcs, which replaces the (fixed) endpoints by (free) large dots. This map C is clearly surjective and the above observation says that it induces a bijective map when working up to w_k–equivalence. But the referee pointed out that the map C itself is not injective. Indeed, the injectivity of C would imply that, for welded long knots, one can, using only arrow moves, delete any w–tree whose head is adjacent to a (fixed) endpoint; but such a sequence would apply likewise to the welded knot obtained by closure, thus basically implying that welded knot theory is trivial.

But, since C is injective up to w_k–equivalence, we have by the same arguments as above that any welded knot is w_k–equivalent to the trivial knot. This is an alternative proof for Theorem 8.1.

10.2 Finite-type invariants of ribbon 2–knots and torus knots

As outlined above, the notion of welded arcs is relevant for the study of ribbon 2–knots in 4–space. Indeed, applying the Tube map to a welded arc, capping off by disks at the endpoints yields a ribbon 2–knot, and any ribbon 2–knot arises in this way [30]. Combining this with the surjective map C from Section 10.1 above, we obtain:

Fact 10.1 *Any ribbon 2–knot can be presented, via the Tube map, by a welded long knot.*

Recall that Habiro introduced in [13] the notion of C_k–equivalence, and more generally the calculus of claspers, and proved that two knots share all finite-type invariants of degree $< k$ if and only if they are C_k–equivalent. As a 4–dimensional analogue of this result, Watanabe introduced in [31] the notion of RC_k–equivalence, and a topological calculus for ribbon 2–knots. He proved the following:

Theorem 10.2 *Two ribbon 2–knots share all finite-type invariants of degree $< k$ if and only if they are RC_k–equivalent.*

We will not recall the definition of the RC_k–equivalence here, but only note the following:

Fact 10.3 *If two welded (long) knots are w_k–equivalent, then their images by the Tube map are RC_k–equivalent.*

This follows from the definitions for $k = 1$ (see Figure 3 of [31]), and can be verified using (E) and Watanabe's moves [31, Figure 6] for higher degrees.

Corollary 8.6 gives a welded version of Theorem 10.2, and can actually be used to reprove it.

Proof of Theorem 10.2 Let R and R' be two ribbon 2–knots and, using Fact 10.1, let K and K' be two welded long knots representing R and R', respectively. If R and R' share all finite-type invariants of degree $< k$, then they have the same normalized coefficients of the Alexander polynomial α_i for $1 < i < k$, by [14]. As seen in Remark 6.1, this means that K and K' have the same α_i for $1 < i < k$, hence are w_k–equivalent by Corollary 8.6. By Fact 10.3, this shows that R and R' are RC_k–equivalent, as desired. (The converse implication is easy; see [31, Lemma 5.7].) □

Using very similar arguments, we now provide quick proofs for the topological consequences of Corollaries 8.6 and 8.2.

Proof of Corollary 8.7 If two ribbon 2–knots have same invariants α_i for $1 < i < k$, then the above argument using Corollary 8.6 shows that they are RC_k–equivalent. This implies that they cannot be distinguished by any finite-type invariant [31, Lemma 5.7].
□

Proof of Corollary 8.3 Let T be a ribbon torus knot. In order to show that T and the trivial torus knot share all finite-type invariants, it suffices to show that they are RC_k–equivalent for any integer k. But this is now clear from Fact 10.3, since any welded knot K such that $\mathrm{Tube}(K) = T$ is w_k–equivalent to the trivial diagram, by Theorem 8.1. □

10.3 Welded string links and universal invariant

We expect that arrow calculus can be successfully used to study welded string links, beyond the homotopy case treated in Section 9. In view of Corollary 8.2, and of Habiro's work in the classical case [13], it is natural to ask whether finite-type invariants of degree $< k$ classify welded string links up to w_k–equivalence. A study of the low-degree cases, using the techniques of [23], seems to support this fact.

A closely related problem is to understand the space of finite-type invariants of welded string links. One can expect that there are essentially no further invariants than those studied in this paper, ie that the normalized Alexander polynomial and welded Milnor invariants together provide a universal finite-type invariant of welded string links. One way to attack this problem, at least in the case of rational-valued invariants, is to relate those invariants to the universal invariant Z^w of Bar-Natan and Dancso [5]. It is actually already shown in [5] that Z^w is equivalent to the normalized Alexander polynomial for welded long knots, and it is very natural to conjecture that the "tree part" of Z^w is equivalent to welded Milnor invariants, in view of the classical case [12]. Observe that, from this perspective, w–trees appear as a natural tool, as they provide a "realization" of the space of oriented diagrams where Z^w takes its values (see also [27]), just like Habiro's claspers realize Jacobi diagrams for classical knotted objects. In this sense, arrow calculus provides the Goussarov–Habiro theory for welded knotted objects.

10.4 w_n–equivalence versus C_n–equivalence

Recall that, for $n \geq 1$, a C_n–move is a local move on knotted objects involving $n+1$ strands, as shown in Figure 42. (A C_1–move is by convention a crossing change.) The C_n–equivalence is the equivalence relation generated by C_n–moves and isotopies.

Proposition 10.4 *For all $n \geq 1$, C_n–equivalence implies w_n–equivalence.*

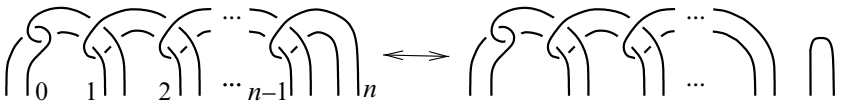

Figure 42: A C_n–move

Proof It suffices to show that a C_n–move can be realized by surgery along w–trees of degree $\geq n$, which is done by induction. It is convenient to use the following notion: given a w–tree T for a diagram with components labeled from 0 to n, the *index* of T is the set of all indices i such that T intersects the i^{th} component of D at some endpoint. We prove the following:

Claim 10.5 *For all $n \geq 1$, the diagram shown in Figure 42, left, is obtained from the $(n+1)$–strand trivial diagram by surgery along a union F_n of* w*–trees such that each component of F_n has index $\{0, 1, \dots, i\}$ for some i.*

Before showing Claim 10.5, let us observe that it implies Proposition 10.4. Note that, if we delete those w–trees in F_n having index $\{0, 1, \dots, n\}$, we obtain a w–tree presentation of Figure 42, right. Such w–trees have degree $\geq n$, and by Lemma 5.9 (inverse), deleting them can be realized by surgery along w–trees of degree $\geq n$. Therefore, we have shown Proposition 10.4.

Let us now turn to the proof of Claim 10.5. The case $n = 1$ is clear, since it was already noted that a crossing change can be achieved by a sequence of (de)virtualization moves or, equivalently, by surgery along w–arrows (see Section 7.2). Now, using the induction hypothesis, consider the following w–tree presentation for the $(n+1)$–strand diagram in Figure 42, left:

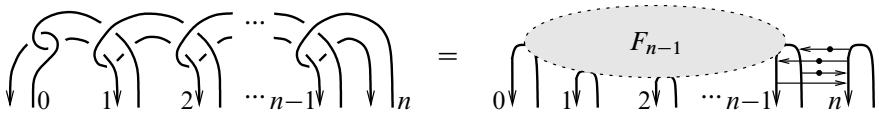

(Here, we have made a choice of orientation of the strands, but it is not hard to check that other choices can be handled similarly.) By moving their endpoints across F_{n-1}, the four depicted w–arrows with index $\{n-1, n\}$ can be canceled pairwise. By Corollary 7.13, moving w–arrow ends across F_{n-1} can be made at the expense of additional w–trees with index $\{0, 1, \dots, n\}$. This completes the induction. □

We note here that, even though C_n–equivalence implies w_n–equivalence, it is not true in general that w_n–equivalence extends C_n–equivalence, in the sense that two

w_n–equivalent classical knotted objects are not necessarily C_n–equivalent. This is for example clear from the case of classical knots, which are all w_n–equivalent by Theorem 8.1, whereas Goussarov–Vassiliev invariants provide several obstructions for their C_n–equivalence.

10.5 Arrow presentations allowing classical crossings

In the definition of an arrow presentation (Definition 4.1), we have restricted ourselves to diagrams with only virtual crossings. Actually, we could relax this condition, and consider more general arrow presentations with both classical and virtual crossings. The inconvenience of this more general setting is that some of the moves involving w–arrows and crossings are not valid in general. For example, although passing a diagram strand *above* a w–arrow tail is a valid move (as one can easily check using the OC move), passing *under* a w–arrow tail is not permitted, as it would violate the forbidden UC move. Note that passing above or under a w–arrow head is allowed. Since one of the main interests of arrow calculus resides, in our opinion, in its simplicity of use, we do not further develop this more general (and delicate) version in this paper.

10.6 Arrow calculus for virtual knotted objects

Although we restricted ourselves to the study of welded (and classical) knotted objects, the main definitions of this paper can be applied verbatim for virtual ones. Specifically, we can use the notions of arrow and w–tree presentations for virtual knotted objects. The main difference is that the corresponding calculus is more constrained, and significantly less simple in practice. Among the six arrow moves of Section 4.3, moves (1), (2), (4) and (5) are still valid, but the tails exchange move (3) is forbidden (we indeed saw that it is essentially equivalent to the OC move); the slide move (6) is not valid in the given form, as the proof also uses the OC move, but a version can be given for virtual diagrams, which is closer in spirit to Gauss diagram versions of the Reidemeister III move. The calculus for w–trees is thus also significantly altered.

The w_k–equivalence relation also makes sense for virtual objects. It is noteworthy that Proposition 7.5 still holds in this context: two virtual knotted objects that are w_k–equivalent, with $k \geq 1$, cannot be distinguished by finite-type invariants of degree $< k$. Indeed, as seen in Section 7.3, the proof is mainly formal, and only uses the definition of w–trees, and more precisely their Brunnian property (Proposition 5.5). It would be interesting to study the converse implication for virtual (long) knots.

From the universal invariant point of view, however, a full virtual extension of arrow calculus should provide a diagrammatic realization of Polyak's algebra [27], which implies a significant enlargement; for example, vertices with one ingoing and two outgoing edges, and the moves involving such w–trees, should be investigated.

References

[1] **B Audoux**, **P Bellingeri**, **J-B Meilhan**, **E Wagner**, *Homotopy classification of ribbon tubes and welded string links*, Ann. Sc. Norm. Super. Pisa Cl. Sci. 17 (2017) 713–761 MR

[2] **B Audoux**, **P Bellingeri**, **J-B Meilhan**, **E Wagner**, *Extensions of some classical local moves on knot diagrams*, Michigan Math. J. 67 (2018) 647–672 MR

[3] **B Audoux**, **J-B Meilhan**, **E Wagner**, *On codimension two embeddings up to link-homotopy*, J. Topol. 10 (2017) 1107–1123 MR

[4] **D Bar-Natan**, *Vassiliev homotopy string link invariants*, J. Knot Theory Ramifications 4 (1995) 13–32 MR

[5] **D Bar-Natan**, **Z Dancso**, *Finite-type invariants of w-knotted objects, I: w-knots and the Alexander polynomial*, Algebr. Geom. Topol. 16 (2016) 1063–1133 MR

[6] **T E Brendle**, **A Hatcher**, *Configuration spaces of rings and wickets*, Comment. Math. Helv. 88 (2013) 131–162 MR

[7] **R Fenn**, **R Rimányi**, **C Rourke**, *The braid-permutation group*, Topology 36 (1997) 123–135 MR

[8] **T Fiedler**, *Gauss diagram invariants for knots and links*, Mathematics and its Applications 532, Kluwer, Dordrecht (2001) MR

[9] **M Goussarov**, **M Polyak**, **O Viro**, *Finite-type invariants of classical and virtual knots*, Topology 39 (2000) 1045–1068 MR

[10] **M Gusarov**, *On n–equivalence of knots and invariants of finite degree*, from "Topology of manifolds and varieties" (O Viro, editor), Adv. Soviet Math. 18, Amer. Math. Soc., Providence, RI (1994) 173–192 MR

[11] **N Habegger**, **X-S Lin**, *The classification of links up to link-homotopy*, J. Amer. Math. Soc. 3 (1990) 389–419 MR

[12] **N Habegger**, **G Masbaum**, *The Kontsevich integral and Milnor's invariants*, Topology 39 (2000) 1253–1289 MR

[13] **K Habiro**, *Claspers and finite type invariants of links*, Geom. Topol. 4 (2000) 1–83 MR

[14] **K Habiro**, **T Kanenobu**, **A Shima**, *Finite type invariants of ribbon 2–knots*, from "Low-dimensional topology" (H Nencka, editor), Contemp. Math. 233, Amer. Math. Soc., Providence, RI (1999) 187–196 MR

[15] **K Habiro**, **J-B Meilhan**, *On the Kontsevich integral of Brunnian links*, Algebr. Geom. Topol. 6 (2006) 1399–1412 MR

[16] **K Habiro**, **A Shima**, *Finite type invariants of ribbon 2–knots, II*, Topology Appl. 111 (2001) 265–287 MR

[17] **A Ichimori**, **T Kanenobu**, *Ribbon torus knots presented by virtual knots with up to four crossings*, J. Knot Theory Ramifications 21 (2012) art. id. 1240005 MR

[18] **T Kanenobu**, *Virtual arc presentations and HC-moves of ribbon 2–knots*, J. Knot Theory Ramifications 11 (2002) 387–402 MR

[19] **T Kanenobu**, **A Shima**, *Two filtrations of ribbon 2–knots*, Topology Appl. 121 (2002) 143–168 MR

[20] **L H Kauffman**, *Virtual knot theory*, European J. Combin. 20 (1999) 663–690 MR

[21] **X-S Lin**, *Power series expansions and invariants of links*, from "Geometric topology" (W H Kazez, editor), AMS/IP Stud. Adv. Math. 2, Amer. Math. Soc., Providence, RI (1997) 184–202 MR

[22] **J-B Meilhan**, **A Yasuhara**, *On C_n–moves for links*, Pacific J. Math. 238 (2008) 119–143 MR

[23] **J-B Meilhan**, **A Yasuhara**, *Characterization of finite type string link invariants of degree < 5*, Math. Proc. Cambridge Philos. Soc. 148 (2010) 439–472 MR

[24] **J Milnor**, *Link groups*, Ann. of Math. 59 (1954) 177–195 MR

[25] **J Milnor**, *Isotopy of links*, from "Algebraic geometry and topology: a symposium in honor of S Lefschetz" (R H Fox, D C Spencer, A W Tucker, editors), Princeton Univ. Press (1957) 280–306 MR

[26] **T Ohtsuki**, *Problems on invariants of knots and 3–manifolds*, from "Invariants of knots and 3–manifolds" (T Ohtsuki, T Kohno, T Le, J Murakami, J Roberts, V Turaev, editors), Geom. Topol. Monogr. 4, Geom. Topol. Publ., Coventry (2002) 377–572 MR

[27] **M Polyak**, *On the algebra of arrow diagrams*, Lett. Math. Phys. 51 (2000) 275–291 MR

[28] **M Polyak**, *Minimal generating sets of Reidemeister moves*, Quantum Topol. 1 (2010) 399–411 MR

[29] **M Polyak**, **O Viro**, *Gauss diagram formulas for Vassiliev invariants*, Int. Math. Res. Not. 1994 (1994) 445–453 MR

[30] **S Satoh**, *Virtual knot presentation of ribbon torus-knots*, J. Knot Theory Ramifications 9 (2000) 531–542 MR

[31] **T Watanabe**, *Clasper-moves among ribbon 2–knots characterizing their finite type invariants*, J. Knot Theory Ramifications 15 (2006) 1163–1199 MR

[32] **T Yajima**, *On the fundamental groups of knotted 2–manifolds in the 4–space*, J. Math. Osaka City Univ. 13 (1962) 63–71 MR

[33] **A Yasuhara**, *Self delta-equivalence for links whose Milnor's isotopy invariants vanish*, Trans. Amer. Math. Soc. 361 (2009) 4721–4749 MR

CNRS, Institut Fourier, Université Grenoble Alpes
Grenoble, France

Faculty of Commerce, Waseda University
Shinjuku-ku, Tokyo, Japan

jean-baptiste.meilhan@univ-grenoble-alpes.fr, yasuhara@waseda.jp

http://www-fourier.ujf-grenoble.fr/~meilhan/

Received: 1 March 2018 Revised: 13 July 2018